INTERACT MEETING REQUEST

and Background Materials for

UW-LNP-ABE8E

Krishanu Saha, PhD

Professor, Department of Biomedical Engineering and Pediatrics

University of Wisconsin-Madison

February 19, 2025

IND Number:	Not Assigned
Product Name:	UW-LNP-ABE8E, including UW-LNP-ABE8E-W53X and UW-LNP-ABE8E-T153I
Investigational Drug Product:	UW-LNP-ABE8E is a novel lipid nanoparticle complex ([redacted]LNP) containing messenger RNA (mRNA) encoding for Adenine Base Editor 8E (ABE8E) and the single guide RNA (sgRNA) targeting the pathogenic W53X or T153I mutation in *KCNJ13*
Route of Administration:	Solution for subretinal injection; single administration
Proposed Regulatory Path:	505(b)(1)
Proposed Indication (s):	Non-end stage Leber Congenital Amaurosis 16 (LCA16), carrying a pathogenic W53X or T153I mutation
Date of Request:	February 19, 2025
Sponsor Contact Name and Contact Information:	Krishanu Saha, PhD Professor, Biomedical Engineering and Pediatrics University of Wisconsin-Madison 330 N. Orchard St. Madison, WI 53715 [redacted]
US Agent Contact Name and Contact Information:	Nicholas P. Shinners, PhD Founder, Principal Consultant Crawling Stone Consulting, LLC 840 Ridgeview Drive Pittsburgh, PA 15228 [redacted]

TABLE OF CONTENTS

LIST OF FIGURES

LIST OF TABLES

ABBREVIATIONS AND ACRONYMS

AAV: Adeno-associated virus
A-Base: Adenine base
ABE8E: A-Base editor 8E
BCVA: Best Corrected Visual Acuity
CBER: Center for Biologics Evaluation and Research
CATT: CBER Advanced Technologies Team
CD_3OD: Deuterated methanol
CPP: Critical process parameters
CQA: Critical quality attributes
Da: Dalton
[redacted]
DRF: Dosage range finding
DLS: Dynamic Light Scattering
[redacted]
ERG: electroretinogram
ESI: Electrospray ionization
ETDRS: Early Treatment of Diabetic Retinopathy Study
FAF: Fundus Autofluorescence
ffERG: Full-field Electroretinography
FIH: First in Human
FST: Full-field stimulus testing
FTIR: Fourier Transform Infrared Spectroscopy
[redacted]
GE: Gene editing
HEK: Human embryonic kidney
HPLC: High-performance liquid chromatography
IE: Ion Exchange
iPSC: induced pluripotent stem cells
ISCEV: International Society for Clinical Electrophysiology of Vision
IRD: Inherited retinal dystrophy
LAL: Limulus Amebocyte Lysate
LCA: Leber Congenital Amaurosis
LNP: Lipid nanoparticle
MLMT: Multi-luminance mobility test

MS: Mass spectrometry
mfERG: multifocal electroretinography
mRNA: messenger RNA
MWCO: Molecular weight cut-off
NMR: Nuclear magnetic resonance
NHP: Nonhuman primates
NOAEL: No Observed Adverse Effect Level
OCT: Optical Coherence Tomography
PEG: Polyethylene glycol
PPM: Parts per million
PR: Photoreceptor
ROA: Route of administration (subretinal injection)
RPE: Retinal pigment epithelium
SCGE: Somatic Cell Genome Editing Consortium
SD-OCT: spectral domain optical coherence tomography
sgRNA: single guide RNA
SNC: Silica nanocapsule
SNV: Single nucleotide variant
SPPS: Solid-phase peptide synthesis

1. EXECUTIVE SUMMARY

Leber Congenital Amaurosis (LCA) is an uncommon cause of severe, early-onset blindness resulting from inherited outer retinal degenerative disease. One form of LCA, LCA16, is caused due to the loss of function of the Kir7.1 potassium ion channel (encoded by the *KCNJ13* gene, location#2q37.1, OMIM#603208). This protein is present in the apical processes of the retinal pigmented epithelium (RPE) cells of the eye. Multiple pathogenic mutations in *KCNJ13* are known to cause LCA16, including adenine base (A-base) mutations resulting in a premature stop codon generated at amino acid 53 (p.W53X; i.e., W53X) and a substitution of threonine to isoleucine at amino acid 153 (p.T153I; i.e., T153I). The Sponsor proposes to repair *KCNJ13* pathogenic A-base mutations using the drug product UW-LNP-ABE8E, a novel lipid nanoparticle (LNP) encapsulated Cas-based adenine base editor (ABE) paired with either a single guide RNA (sgRNA) targeting *KCNJ13* mutation W53X or sgRNA targeting mutation T153I. These drug substances will be delivered to the RPE of LCA16 patients via subretinal injection.

LCA16 is an ultra-rare condition, with about 21 patients identified worldwide to date. However, it is very likely that more patients exist who are not currently in accessible databases, such that more subjects could become available to participate once a therapeutic trial is made known. Within the group of known patients, one has been identified with the W53X mutation and four with the T153I mutation, all of whom are between the ages of 12 and 22. Because LCA16 is a progressive retinal dystrophy, with vision loss and irreversible death of RPE later in adulthood, UW-LNP-ABE8E is targeted to treat patients in whom some RPE cell patches are intact (as determined by standard imaging techniques such as Optical Coherence Tomography, or OCT, and fundus autofluorescence, or FAF). The combination of a very low disease prevalence and the need to treat younger patients means that the available population for the generation of clinical safety and efficacy data is not only currently limited but will continue to be very limited going forward. Given the rarity of the disease, the development of the UW-LNP-ABE8E clinical program is challenging. However, the Sponsor believes these challenges are offset by the likelihood that UW-LNP-ABE8E can make a profound and permanent impact on the vision of these affected individuals who currently have no other approved treatment. More specifically, in vitro and in vivo proof-of-concept data demonstrate that base correction of a W53X mutation in the RPE of a *KCNJ13* mutant

mouse and in a patient-derived model, the human *KCNJ13* W53X mutant iPSC-RPE, can halt progressive retinal degeneration and restore Kir7.1 channel function, leading to a measurable restoration of electroretinogram (ERG) c-wave (an indication of functional RPE cells), and improvement in visual function.

Because multiple mutations in *KCNJ13* can cause LCA16, the Sponsor proposes to repair the *KCNJ13* gene via a platform approach. The target cell type (RPE), therapeutic deoxyadenosine deaminase base editor (ABE8E), delivery vehicle (LNP), route of administration (ROA; subretinal injection), and dose will remain constant, while the DNA-targeting, Cas-sgRNA ribonucleoprotein changes as different mutation sites are targeted. The Cas-sgRNA ribonucleoprotein fused to the deoxyadenosine deaminase, TadA-8e, binds and targets the patient's DNA. ABE8E has been shown to be active with various Cas homologs, including Cas9 and Cas12 ribonucleoproteins containing sgRNA sequences targeting diverse mutations. The inclusion of two pathogenic mutations as targets within *KCNJ13* will allow the design of a product that will impact more patients presenting with LCA16 and provide the framework for the application of a manufacturing and nonclinical approach that will be valuable across additional pathogenic mutations not only for LCA16, but also many other diseases of the RPE, as well as several other diseases caused by similar monogenetic A-base mutations.

The Sponsor is seeking early input from the FDA on the proposed chemistry, manufacturing and controls (CMC) and nonclinical development program for UW-LNP-ABE8E to support a first-in-human clinical trial (FIH) in patients with non-end stage LCA16 carrying a pathogenic W53X or T153I mutation. In addition, the Sponsor seeks input from the Agency on the proposed use of a platform technology approach to treating a single disease indication with unique drug products that differ only in the sequence of their sgRNA and a nominally altered Cas homolog. There are no previous or currently existing marketing authorizations or authorization applications for UW-LNP-ABE8E. UW-LNP-ABE8E has not yet been administered to humans. To date, there have been no meetings with Health Authorities to discuss UW-LNP-ABE8E.

2. PRODUCT DEVELOPMENT OVERVIEW

2.1. Disease Background

LCA is an uncommon cause of severe, early-onset blindness resulting from inherited outer retinal degenerative disease.[1,2] Some of the typical phenotypes of LCA include pigmentary changes, nystagmus, photophobia, and reduced or no recordable ERG waveforms. LCA16 (OMIM#614186) is a severe autosomal recessive inherited retinal dystrophy (IRD) leading to blindness in early life. LCA16 is caused by the loss of function of the Kir7.1 potassium ion channel (encoded by the *KCNJ13* gene, location#2q37.1, OMIM#603208) in the apical processes of the RPE (**Figure 1**) cells of the eye[1].

Figure 1 Subretinal injection into the eye targeting RPE

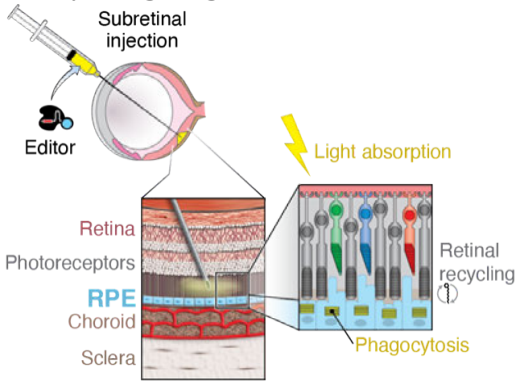

Legend: Injecting into the subretinal space localizes the dose proximal to the retinal pigmented epithelium (RPE). Anatomy of the eye, highlighting the blood-retina barrier of the RPE and crosstalk with photoreceptors during phototransduction. Adapted from DiCarlo et al.[3]

The Kir7.1 channel controls K+ homeostasis in the subretinal space, supporting photoreceptor-RPE cell-cell signaling in support of visual functions such as phototransduction and phagocytosis. Several missense and nonsense loss-of-function mutations have been reported in *KCNJ13*, leading to diminished K+ conductance of the RPE and altered ERG[4–12]. Our therapeutic approach lies with the structure/function relationship of Kir7.1, in which making the functional Kir7.1 channel enables the K+ conductance of RPE to resume and restore photoreceptor function (**Figure 2**). The Sponsor has developed a novel LNP-delivered CRISPR base editor mRNA and sgRNA to RPE to correct mutations in *KCNJ13* known to cause a subtype of LCA, called LCA16.

Because multiple mutations in *KCNJ13* can cause LCA16, the Sponsor proposes to create a program to repair the *KCNJ13* gene using a Cas-based A-Base editor, ABE. Additionally, the target cell type (RPE), base editor (ABE8E), delivery vehicle (LNP), ROA, and dose will remain constant as different mutation sites are targeted, while the Cas-sgRNA ribonucleoprotein changes. The inclusion of targets of two pathogenic mutations within *KCNJ13* — a premature stop codon generated at amino acid 53 (p.W53X; i.e., W53X) and a substitution of threonine to isoleucine at amino acid 153 (p.T153I; i.e., T153I) (**Figure 3**) — will allow us to design a product that will impact more patients presenting with LCA16 and provide the framework for the use of a manufacturing and nonclinical approach that will be valuable across many diseases of the RPE. The Sponsor is seeking feedback on the design of this platform-based approach through this INTERACT Meeting.

2.2. Current Practice and Limitations

As of now, there is no approved therapy that can treat LCA16 blindness. There is one gene therapy program in development that aims to overexpress the wildtype *KCNJ13* coding sequencing via adeno-associated viral (AAV) vector delivery to the subretinal space (Hubble Therapeutics, HUB-101). This program is in the preclinical stages of development.

2.3. Product Rationale

Gene Editing Approach to Treat LCA16

RPE is an epithelial monolayer of polarized cells with tight junctions that form an essential blood-retina barrier for solutes, nutrients, and other molecules and provide critical support for photoreceptor (PR) cells. Therefore, impairment of RPE functions includes abnormalities in 1) the formation of a tight blood-retina barrier, 2) phagocytosis and recycling of PR membrane components, 3) daily regeneration of visual pigments, 4) supply of nutrients to the PR, and 5) maintenance of ionic homeostasis in the PR environment by ion transport mechanisms[13–15].

The nonsense mutation variant c.158G>A (W53X) causes LCA16 via loss-of-function of the Kir7.1 ion channel[2]. Similarly, a missense variant c.458C>T (T153I) alters the pore structure to inhibit K+-ion permeation[16]. Gene editing is expected to correct the endogenous gene and would reverse the underlying cause of the disease by restoring the function of Kir7.1 and re-establishing normal ionic gradient across the RPE (**Figure 2**).

Figure 2 Kir7.1 ion channel maintains K+ gradient across RPE

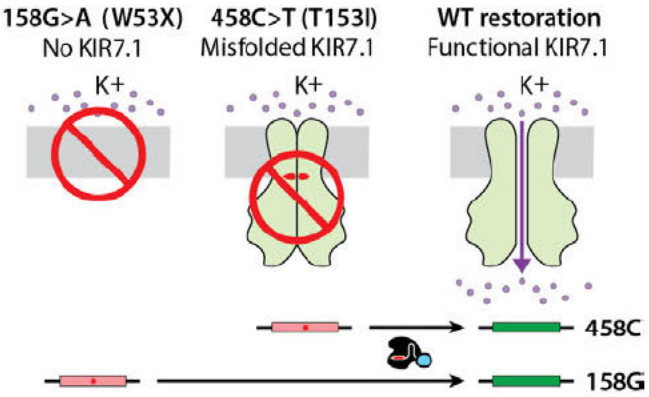

Legend: Restoration of Kir7.1 channel function through A-base editing of *KCNJ13* is expected to restore RPE and photoreceptor function.

Intended Mechanism of Action

The W53X mutation within *KCNJ13* disrupts Kir7.1 channel production via a nonsense G>A mutation that results in a premature stop codon (**Figure 3**). This nonsense point mutation is ideal for treatment using an adenine base editor to restore the intended sequence and remove the premature stop, thereby restoring the production of Kir7.1. The Sponsor has conducted proof-of-concept experiments delivering messenger RNA (mRNA) encoding for an adenine base editor, ABE8E[17,18] (ABE8E), along with a sgRNA for the W53X mutation utilizing a LNP-based delivery system. These experiments demonstrated the rescue of the Kir7.1 potassium channel function in RPE cells that contain the W53X mutation and a measurable restoration of RPE function. Furthermore, the Cas9-sgRNA ribonucleoprotein has been designed to target the A-base T153I mutation with the same ABE8E editor, which will repair the pore structure of Kir7.1 channel to facilitate normal ion conduction.[16]

While most gene therapies, such as LUXTURNA®, rely on viral delivery systems (AAV vectors), these systems pose risks, including dysregulated transgene expression and immunogenicity, along with challenges associated with limited cargo capacity and manufacturing difficulties[19–21]. As a result, the Sponsor has opted for an LNP-based delivery system, which offers several key advantages. Namely, LNPs can encapsulate larger payloads, making them well-suited for the transient delivery of large, complex gene-editing machinery, such as ABE8E and sgRNA. Additionally, their composition allows for easier manufacturing and scalability, making them an ideal alternative for gene therapy delivery [22–24].

Figure 3 Pathogenic *KCNJ13* mutations to be targeted by UW-LNP-ABE8E

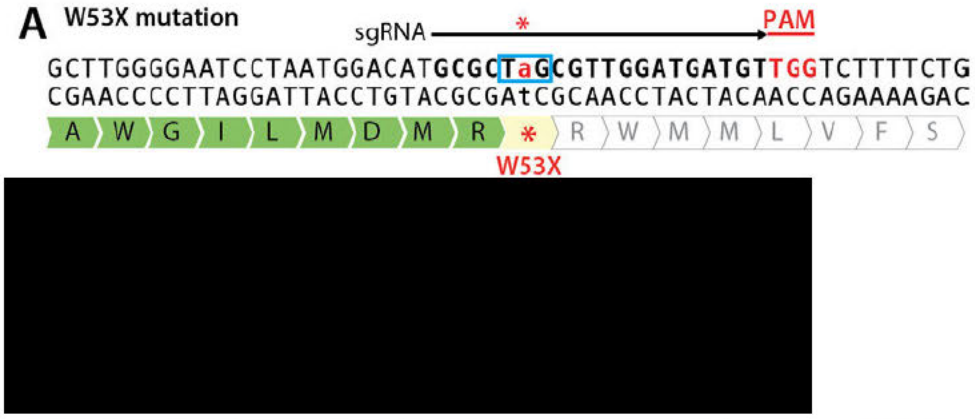

Legend: **A.** c.158G>A, W53X (SPDI: NC_000002.12:232771204:C:T). **B.** c.458C>T, T153I (SPDI:

NC_000002.12:232768407:A:G). The mutant codon is marked with a blue box and translated amino acids are below. Position of the W53X and T153I targeting sgRNAs are shown with black line and corresponding PAM with red line.

Subretinal injection into the space between the neural retina layer and RPE (**Figure 1**) can largely restrict a genome editing drug to the retinal side of this blood-retina barrier.[25] Therefore, the biodistribution of the injected drug is localized, specifically next to the RPE that phagocytoses fluid from the subretinal space. Safety issues with subretinal injection are expected to be significantly lower than attempting to dose via systemic delivery through the bloodstream.

In a murine model of LCA16, a single dose of ABE8E (3 µg) delivered via nanoparticles through the intended subretinal ROA resulted in measurable improvements in visual function recorded via multifocal electroretinography (mfERG) over 10 weeks, achieving a 17±8% on-target editing efficiency of the W53X mutant allele.[26] The Sponsor plans to conduct dose-ranging studies in future small animal testing to establish the dosing regimen for UW-LNP-ABE8E for the FIH study, with the minimum dose needed to achieve measurable improvement in retinal function serving as the threshold for the lowest dose. The dose that achieves the greatest improvement in retinal function will be the highest dose, assuming a similar safety profile. Each dose of UW-LNP-ABE8E in an LCA16 patient is anticipated to cover approximately 6% of the entire human retina (64 mm^2 for a 9 mm diameter bleb from subretinal injections within a total area of 1094 mm^2 of the human retina). With standard guidance of the injection needle by the surgeon, the administered dose within 100 µL of volume specifically targeting the macula is expected to encompass the entire macula area (5 mm in diameter), leading to durable gene correction and improvements in both central vision and possibly peripheral vision. Two additional injections at the retina's periphery, each with a single dose of 100 µL volume taken from single-use vials, are expected to enhance peripheral vision. Overall, up to three subretinal doses could be administered to a single eye of a LCA16 patient in a surgery, which cumulatively would cover about 20% of the retina.

3. PROGRAM STATUS

The Sponsor has conducted studies encompassing the efficacy of ABE8E for the treatment of LCA16 and the development of a novel nanoparticle delivery system using a novel lipopeptide, guanidinium-rich lipopeptide [redacted] as a part of the nanoparticle structure. Our efforts are currently focused on development to support the submission of an IND. This work spans multiple areas critical to development, including preliminary proof-of-concept studies in LCA16 patient-derived iPSC-RPE cells and rodent disease models. We are planning additional nonclinical studies, development of manufacturing capability for UW-LNP-ABE8E, transfer of manufacturing capability to a Phase-appropriate manufacturing facility, and initial plans for clinical trial design.

The Sponsor is a part of the National Institutes of Health Somatic Cell Genome Editing (SCGE) consortium and has had preliminary interaction with Center for Biologics Evaluation and Research (CBER) through that affiliation. Specifically, the Sponsor participated in the consortium's meeting with the CBER Advanced Technologies Team (CATT), which occurred on March 12, 2024, in which the point of discussion was the design of a platform to identify and verify off-target sites for RNA-guided genome editors. The concepts discussed during that meeting have been used to structure the proposed off-target editing analysis for UW-LNP-ABE8E, although the specific data and off-target analysis plan included in this briefing book has not been discussed with CBER.

As a member of the SCGE, we are aware of the INTERACT meeting submissions from other member sponsors, including that from Dr. Musunuru and Dr. Ahrens-Nicklas of the University of Pennsylvania and the Pennsylvania Children's Hospital, and from Dr. Yong-hui Jiang of Yale University. The SCGE and generosity of our colleagues has enabled us to share results and feedback from these meetings with one another, which has informed our meeting package and development plan. However, our project differs from those projects in important ways that necessitate this INTERACT meeting. Specifically, the development of a novel component to the LNP is unique to our work, and requires guidance from the Agency. Moreover, the eye is a unique organ for treatment, with its own

challenges and advantages for somatic cell genome editing, requiring additional feedback. As with the other members of the SCGE, we plan to disseminate this submission and feedback obtained, after redacting confidential information, with the other members of the consortium.

4. LIST OF SPECIFIC QUESTIONS BY DISCIPLINE

4.1. Chemistry, Manufacturing and Controls (CMC)

4.1.1. Question 1: Novel Excipient

Does the Agency agree that the [redacted] used in the manufacturing process is of sufficient quality for a First in Human (FIH) Trial?

Sponsor Position

A detailed description of the synthesis of the [redacted] is shown in Section 5.2 and **Figure 20**. The Sponsor intends to ensure that the quality of the [redacted] is sufficient for use in definitive GLP animal studies and clinical studies by transferring the manufacturing process to a CDMO. We will define critical quality attributes (CQA) as described in **Table 7** to confirm the identity and purity of the [redacted] material. Additional development experiments will be performed to assess the purity necessary to prevent cytotoxicity and maintain LNP encapsulation and loading of RNA. The Sponsor will also conduct thorough biodistribution studies to evaluate tissues in which [redacted] may accumulate, including, but not limited to, the liver, lungs, heart, brain, gonads, and kidneys.

[redacted] is added to the drug substance (DS) as a part of the final drug product (DP) manufacturing and accounts for 50 mol% of the lipid components of the LNP delivery vehicle (**Table 10**). The LNP delivers the ABE8E mRNA and sgRNA to the target RPE cells, causing the corrective editing of the W53X allele in the *KCNJ13* gene. The therapeutic effect is therefore not mediated through the [redacted] or other components of the lipid nanoparticle, but rather the DS consisting of the ABE8E mRNA and sgRNA. The Sponsor's position is that the [redacted] does not make up a critical component of the DS and may be supplied as a non-GMP material, provided that it is accompanied by a Certificate of Analysis detailing acceptable quality standards.

4.1.2. Question 2: Excipients

Does the Agency agree that the excipients that make up the LNP, other than [redacted] proposed for use in the manufacturing process are of sufficient quality for a FIH Trial?

Sponsor Position

The LNP is composed of [redacted]. The LNP delivers the ABE8E mRNA and sgRNA to RPE cells, causing the corrective editing of the W53X allele on the *KCNJ13* gene. The therapeutic effect of the drug is not mediated through the lipid components of the LNP, but rather the DS consisting of the ABE8E mRNA and sgRNA. The Sponsor's position is that the additional LNP lipid components do not make up a critical component of the DS and may be supplied as a non-GMP material, provided that the DS is accompanied by a Certificate of Analysis detailing acceptable quality standards. Certificates of Analysis will be documented and retained for any materials used for nonclinical studies that support IND submission. These lipid components will be tested and released for use in a GMP-compliant manufacturing facility. The manufacturing process for the DP will then be completed in a GMP setting, including lot release and quality control standards. The Sponsor position is that this level of quality

is sufficient for these excipients to be used to manufacture the UW-LNP-ABE8E DP, and that it is not necessary to source these materials from a GMP manufacturing process.

4.1.3. Question 3: Quality and Characterization Testing

Does the Agency agree that the proposed characterization and release tests are appropriate to control the quality attributes of the excipients, DS and DP for FIH trial?

Sponsor Position

The DP consists of an LNP encapsulating RNA encoding for the DS — mRNA for ABE8E and sgRNA targeting the *KCNJ13* W53X mutation or the T153I mutation. The DP will be assembled through fluidic mixing by a CDMO in accordance with current Good Manufacturing Practices (cGMP). The manufacturing process (**Figure 18**) is designed with processes in place to maintain the safety, purity, identity, and potency of each UW-LNP-ABE8E product. Materials to be used will be phase appropriate (**Table 6**) and facilities maintained at an appropriate cGMP level. The proposed release testing of the DP is shown in **Table 13**, and proposed release testing of cGMP-quality DS sgRNA and ABE8E in **Table 11** and **Table 12**, respectively.

[redacted] (**Table 6**) are commonly used in other drug delivery systems. These materials will be manufactured by industry-recognized vendors. The release testing and specifications will be discussed with the vendors to ensure that the materials will be of high quality and to be provided with the necessary documentation to warrant use in early phase clinical investigation. [redacted] will be outsource manufactured by a CDMO and characterized by a combination of methods to ensure identity and purity (**Table 7**). Process development and further refinement of characterization testing will be critical for the identification and establishment of additional CQAs and critical process parameters (CPP). [redacted] release specifications based on these emerging CQAs and CPPs will be included in the pre-IND package.

4.2. Non-Clinical Proof of Concept

4.2.1. Question 4: Non-clinical off-target analysis

Does the Agency agree that the proposed off-target editing studies are adequate and that there are no anticipated further requirements for analysis of off-target editing to support a FIH clinical trial with UW-LNP-ABE8E?

Sponsor Position

The general strategy for off-target assessment associated with our nonviral base editor therapeutic includes *in silico* prediction, biochemical assays, cell-free and human cell-based assays, and copy number variant analysis for potential off-target events at different levels of genomic resolution. The employment of these methods can be categorized into two phases; the nomination phase and the verification phase. The nomination phase encompasses *in silico* and cellular methods, while the verification phase encompasses targeted sequencing assays. Additionally, we plan to assess genome integrity at the level of large-size structural variants, indels, and single nucleotide variants (SNVs). The Sponsor will perform long-read sequencing to assess intermediate-size structural variants. For the assessment of SNVs and indels, *in silico* analysis using Cas-OFFinder and CHANGE-seqBE in genomic DNA from iPSCs of LCA16 patients and healthy donors will be performed to nominate 100-1000 off-target sites. Nominated off-target sites will be analyzed bioinformatically to examine the clinical relevance of these sites against the 1,000 Genomes and ClinVar databases. We will use the results from these analyses to rank the priority of nominated sites for the verification phase.

We propose to use rhAmpSeq™ CRISPR Multiplexed Amplicon Sequencing & Analysis method and hybrid capture followed by short-read Illumina sequencing for site verification in iPSC-derived RPE from patients and

healthy donors. For the evaluation of specific off-target events, targeted amplicon sequencing will be considered. If warranted, the application of targeted or genome-wide transcriptome analysis and additional off-target screening methods such as CIRCLE-Seq may be considered. The impact of genomic variation on off-target editing will be considered using CRISPRme or other similar programs. A description of the Sponsor's proposed plan is provided in Section 5.1.7. The Sponsor position is that this represents an adequate battery of assays for the nomination and validation of off-target editing sites to assess the off-target toxicity profile for UW-LNP-ABE8E targeted to each mutation (e.g., UW-LNP-ABE8E-W53X or UW-LNP-ABE8E-T153I).

4.2.2. Question 5: Non-clinical Proof of Concept

For each mutation (W53X and T153I), does the Agency agree that assessment of the in vitro on-target editing and in vitro functional recovery of patient-derived iPSC-RPE cells after treatment with UW-LNP-ABE8E are sufficient proof-of-concept studies to support the proposed mechanism of action and a FIH clinical trial for UW-LNP-ABE8E?

Sponsor Position

The Sponsor has developed cell-based assays to support the design of UW-LNP-ABE8E. Notably, patient-derived iPSC-RPE$^{W53X/W53X}$ cells were produced that carry the W53X mutation and demonstrate biomarkers of the LCA16 phenotype, as discussed in Section 5.1.8. When treated with the DS ABE8E mRNA and sgRNA, successful editing was confirmed by short-read Illumina and long-read Oxford Nanopore genetic sequencing. This correction to the *KCNJ13* gene resulted in measurable changes in single-cell conductance in individual cells, as measured by the patch clamp assay described in Section 5.1.6, a direct measure of Kir7.1 function. The Sponsor Position is that these cell-based assays are sufficient to serve as models of LCA16, and the combination of cell-based assays will serve as proof-of-concept for the proposed mechanism of action for UW-LNP-ABE8E to treat LCA16.

4.2.3. Question 6: Potency Assurance

Does the Agency agree that the novel reporter cell line is a viable quality control measure and agree with its use as a release assay for UW-LNP-ABE8E?

Sponsor Position

The Sponsor has developed a novel genetic construct for creating a "reporter" fluorescent cell line with the genetic mutation of interest in LCA16. The design of this construct includes a constitutive enhanced Green Fluorescent Protein (eGFP) fluorophore, and the section of *KCNJ13* genomic target containing either the W53X or T153I target mutation linked to a monomer Red Fluorescent Protein (mRFP) fluorophore.

For W53X, because the target mutation W53X contains a premature stop codon, full length protein is not produced. Therefore, untreated cells in which the W53X mutation has not been corrected do not express the reporter mRFP, resulting in no red fluorescence in the cells. Once the corrective edit is made, the premature stop is removed and full-length protein is restored, including production of mRFP with red fluorescence signal in flow cytometry and fluorescence microscopy assays. In an initial proof-of-concept study, we created a cell line, HepG2^{W53X}, to test the ability of the DP, UW-LNP-ABE8E, to make the intended correction to the target gene. A similar fluorescence reporter has been designed for the T153I mutation. UW-LNP-ABE8E demonstrated the ability to make the intended edit at the target site, resulting in detectable mRFP expressed in treated cells (See **Figure 15**). In order to create a cell-based assay that may be used as a rapid, binary indicator of UW-LNP-ABE8E's editing capability, a reporter assay will be created using this concept in a stable cell line.

The Sponsor intends to use this novel cell-based assay as a lot release criterion and indicator of quality in the production of UW-LNP-ABE8E. The readout for this assay is binary, with eGFP positive and mRFP negative (eGFP^{+}/mRFP^{-}) cells as the baseline condition. After on-target editing at the W53X locus in the transgene, these

cells produce mRFP and become $eGFP^{+}/mRFP^{+}$. This assay will be used as a confirmation that the DS components of UW-LNP-ABE8E are capable of making the intended on-target edit at the target mutation. The sponsor does not intend to use this assay as a quantitative measure of on-target editing or editing efficiency.
The Sponsor's position is that the proof-of-concept $HepG2^{W53X}$ cell line that we have developed and tested is sufficient evidence that this reporter cell line concept is capable of serving as a binary indication of on-target editing. We are in the process of developing a human embryonic kidney (HEK) cell line to stably express the described construct (HEK^{W53X}) based on this concept and will use that assay as a quality measure to confirm the on-target editing capability of the DS. This reporter assay is intended to serve as a lot release test for UW-LNP-W53X and may also be used for stability evaluation and comparability studies. As the UW-LNP-ABE8E manufacturing process is refined, a matrix of product characterization testing shall identify CQAs and CPPs with the goal of establishing a relationship between the test article's mechanism of action (MoA) and potency-related CQAs. As the program matures, in-process and lot-release testing will be included to round out a robust potency assurance strategy. The goal of ongoing potency assay development is to qualify an assay that is specific and ensures that every lot of released DP will have the potency necessary to achieve the intended therapeutic effect.

4.2.4 Question 7: Animal Model Selection

Does the Agency agree that the selection and proposed animal model species selection and design are acceptable for supporting a FIH clinical trial?

Sponsor Position

The Sponsor proposes to conduct the proof-of-concept efficacy and nonclinical safety assessment of UW-LNP-ABE8E in mice as described in Section 5.1. We have designed and created a population of mice heterozygous for the W53X mutation at *KCNJ13*. Unlike in humans, the homozygous W53X mutation in mice is fatal at post-birth day one. The Sponsor has developed a method to treat the RPE of heterozygous $Kcnj13^{W53X/+}$ mice with Cas9 and a sgRNA targeted to the WT locus that interrupts the expression of functional Kir7.1. These $Kcnj13^{W53X/+\Delta R}$ mice lose WT Kir7.1 expression and display reduced c-wave amplitude as measured by ERG, a hallmark of the nonfunctional RPE cells in LCA16. The sponsor has demonstrated that the ABE8E mRNA and an analogous mouse sgRNA in UW-LNP-ABE8E can correctively edit the mutation in $Kcnj13^{W53X/+\Delta R}$ mice, resulting in the restoration of RPE function as indicated by the progressive increase in c-wave amplitude.

Further nonclinical safety and biodistribution studies in a large animal model will be conducted in nonhuman primates (NHP), as described in **Table 3**. NHP will provide crucial biodistribution data in an animal model with anatomical characteristics similar to those in humans. Both acute local and systemic toxicity and immunogenicity data collected in NHP will be used to inform the proposed clinical drug product and route of administration. The Sponsor position is that the described animal models and studies represent an adequate nonclinical testing plan for developing UW-LNP-ABE8E. The Sponsor proposes to use these animal models to enable and inform the design of subsequent, definitive nonclinical and clinical studies.

4.3. Non-Clinical Safety

4.3.1. Question 8: Safety, Pharmacology, and Reproductive Toxicity Assessment

Does the Agency agree that the proposed DP does not constitute a significant risk of germline editing, and that the proposed biodistribution studies are sufficient to eliminate the potential for germline transmission?

Sponsor Position

The Sponsor intends to deliver UW-LNP-ABE8E directly to the eyes of patients with LCA16 via subretinal injection. We have conducted a risk assessment analysis to determine the overall risk factor for generational

germline transmission, which includes a discussion of the amount of material being delivered, the ROA, the potential off-target editing sites for the combination of base editor and guide, and the biodistribution of the drug product's components after delivery in animal models.

The proposed total volume of injected material in humans is up to 300 µL per eye, with a combined total of up to 300 µg of the ABE8E mRNA and sgRNA, which make up the DS. This is significantly less material than in other analogous gene editing applications, where the systemic delivery of LNP or AAV are administered at >10-fold higher doses of DS (microgram scale dosing in the eye versus milligram dosing in systemic delivery), resulting in higher concentrations of the DS in the bloodstream.

The blood-retina barrier in healthy eyes has limited permeability to small molecules, and particles above 2 nm threshold in size do not permeate the RPE well[27]. In the LCA16 murine model, we did not detect any leakage of material across the blood-retina barrier. Furthermore, we have limited evidence of choroidal vasculature degeneration in late-stage LCA16 patients in the clinic with severe retinal vascular attenuation and some areas of neovascularization. The LNPs that comprise UW-LNP-ABE8E, as well as the gene-editing components that make up the DS, have diameters well above this size threshold, and therefore we believe will have limited permeability into the bloodstream.

The Sponsor plans to conduct biodistribution studies in mice (**Table 3**) to observe whether the DS and/or components of the LNP accumulate in the gonads in measurable quantities.

Based on the above, the Sponsor position is that the likelihood of a germline editing event is low. The DS is delivered in a small amount to the eye, which has a low vascular permeability and inhibits widespread distribution. Nominative off-target studies have demonstrated few genomic off-target editing sites without any sites that represent a cause for concern. A longitudinal germline transmission study is therefore not necessary, pending the results of the biodistribution study and assuming that DS/DP components and editing events are not detectable in the mouse gonad tissues.

4.4. Clinical

4.4.1. Question 9: Clinical Trial Design

Does the Agency support a clinical trial design recruiting two patient groups, in which the biodistribution for UW-LNP-ABE8E-W53X and *in vitro* efficacy data for UW-LNP-ABE8E-W53X or UW-LNP-ABE8E-T153I will be used to support the inclusion of patients harboring either the W53X or T153I mutation, and in which either UW-LNP-ABE8E-W53X or UW-LNP-ABE8E-T153I will be administered?

Sponsor Position

The Sponsor plans to conduct an open-label clinical trial of UW-LNP-ABE8E with patients harboring either the W53X or the T153I mutation, conducted in parallel with one another. LCA16 is caused by mutations in the *KCNJ13* gene that lead to the disruption of Kir7.1 ion channels present in the RPE. Kir7.1 controls K^+ homeostasis in the subretinal space, supporting photoreceptor-RPE cell-cell signaling in support of visual functions, such as phototransduction and phagocytosis. There are several reported loss-of-function mutations in *KCNJ13*, which lead to diminished K^+ conductance and altered ERG of the RPE. The mutations W53X and T153I may both be treated through A-base editing at the mutation site (**Figure 3**), and in both cases, correction of the mutation results in normal Kir7.1 function.[16,26] UW-LNP-ABE8E-W53X and UW-LNP-ABE8E-T153I are identical to one another in disease population (LCA16), LNP formulation, therapeutic deoxyadenosine deaminase base editor, and mechanism of action, only differing in the identity of the genomic target recognition portions of the formulation the sgRNA and Cas homolog. The Sponsor position is that UW-LNP-ABE8E-W53X and UW-LNP-ABE8E-T153I be included in a clinical trial, where the patient population with LCA16 is a combined

pool of individuals with the W53X and T153I mutations in the *KCNJ13* gene, will be sufficient to assess the safety of both variants of UW-LNP-ABE8E.

4.4.2. Question 10: Clinical Trial Protocol Amendment

Does the Agency agree that demonstrating benefit in the FIH clinical trial targeting either W53X or T153I mutations would potentially support the amendment of this proposed clinical protocol for UW-LNP-ABE8E to include patients with other pathogenic *KCNJ13* A-base mutations in this ultra-rare, serious disease that results in irreversible loss of vision?

Sponsor Position

Due to the ultra-rare nature of the disease, the feasibility of powering a FIH Phase I clinical trial with patients from a single genotype is not feasible. Therefore, to conduct a Phase II or III trial powered sufficiently to generate generalizable safety and efficacy knowledge, the Sponsor position is that UW-LNP-ABE8E could be expanded to additional pathogenic A-base mutations targetable by ABE8E. Knowledge of the natural history of this ultra-rare disease indicates that LCA16 manifests as a single disease and is diagnosed by, among other modalities, identifying pathogenic mutations in the *KCNJ13* gene. Accordingly, clinical outcome assessments will be shared across the varying pathogenic mutations (both including and beyond W53X and T153I) within a well-defined patient population. As the mechanism of action, biodistribution and cGMP manufacturing process for any new UW-LNP-ABE8E DP targeting these additional pathogenic mutations remain the same, the Sponsor considers these future formulations as potentially comparable to the currently described UW-LNP-ABE8E. After demonstrating benefit with the FIH human trial with W53X or T153I, the Sponsor plans to amend the clinical trial protocol and conduct a clinical trial of UW-LNP-ABE8E with patients harboring additional mutations that have sufficient nonclinical, proof-of-concept studies supporting the benefit of UW-LNP-ABE8E.

5. BACKGROUND INFORMATION

5.1. Nonclinical Background

5.1.1. Design and Selection of sgRNA to target W53X

The Sponsor's approach to the treatment of the LCA16 relies on the use of a base editor to correct the premature stop codon in the W53X mutation. Base editors are engineered proteins that use the programmable DNA targeting ability of Cas9 to bring a nucleotide base-modifying enzyme to an editing window at the target DNA site. This leads to the targeted conversion of one or more bases, resulting in an altered DNA sequence without requiring double strand breaks (DSB) or relying on cellular DNA repair machinery. Since LCA16 is caused by the W53X mutation, c.158G>A nucleotide change, an ABE-mediated base editing strategy can potentially correct the mutation through an A>G conversion.

The Sponsor used three bioinformatic tools for sgRNA design. The sgRNAs targeting the W53X location in the human *KCNJ13* gene were designed using Benchling (https://www.benchling.com) for various Cas homologs.[17,18,28] The design was validated with two other online tools, CRISPR-RGEN [3,4], and PnB Designer [4], to confirm its on-target specificity. Only one sgRNA (**Table 1**) appeared to be very specific for the W53X location as it would allow the binding of the *Sp*Cas9 ribonucleoprotein to the target locus that positions c.158G>A site within the editing window of ABE (4-8 for ABE8E, counting the PAM as 21-23). This sgRNA also had the highest on-target score (65.7) and lowest off-target score (56.8) among the Benchling-designed sgRNAs. The sgRNA targeting mouse *Kcnj13* was also selected based on the above criteria (highest on-target score; 57.1, lowest off-target score; 56.8). [redacted]

Table 1 On-target editing efficiency by ABE8E

KCNJ13 mutation	Species	Model	Delivery	sgRNA protospacer	Cas9 Homolog	% Editing Efficiency
	Mouse	RPE: subretinal, in vivo	Nanoparticles	[redacted]	*Sp*	17 ±8
	Human	LCA16 fibroblasts	Nanoparticles		*Sp*	52.3 ±0.1
	Human	LCA16 iPSC-RPE	Nanoparticles		*Sp*	16.8 ±7.9
	Human	HEK293 Flp	Electroporation		*Sp*	53.0 ±1.4
	Human	HEK293 Flp	Electroporation		*Sauri*	22 ±5
W53X TAG>TGG	Human	HEK293 Flp	Electroporation		*SaKKH*	22 ±8
	Human	HEK293 Flp	Electroporation		*Sauri*	12 ±12
	Human	HEK293 Flp	Electroporation		*eNme2-C*	10 ±9
	Human	HEK293 Flp	Electroporation		*SaKKH*	0.29 ±0.03
	Human	HEK293 Flp	Electroporation		*Sauri*	0.79 ±0.28
	Human	HEK293 Flp	Electroporation		*Sauri*	0.86 ±1.16
	Human	HEK293 Flp	Electroporation		*eNme2-C*	0 ±0
T153I ATA>ACA	Human	LCA16 fibroblasts	Electroporation		*eNme2-C*	14.45 ±3.46
	Human	LCA16 fibroblasts	Electroporation		*eNme2-C*	15.7 ±0.82

Legend: Efficiency of the editor to correct W53X or T153I *KCNJ13* alleles in patient-derived cell models and within mice. Model refers to patient-derived fibroblasts, patient-derived iPSC-RPE, HEK293-Flp or CHO K1 FRT stable cells. Cas Homologs: *Sp*, *Streptococcus pyogenes*; Sauri, *Staphylococcus auricularis*; *eNme-C*: evolved variant *Neisseria meningitidis*; *SaKKH*, KKH variant of *Staphylococcus aureus*. T153I editing efficiency is based on mutation correction without bystander nucleotide editing affecting splicing.

Single guide RNAs are essential for gene editing, as they direct the ABE8E editor to specific target sequences within the genome. To improve both the stability and efficiency of the sgRNA, chemical modifications such as 2'-O-methyl and phosphorothioate linkages are introduced at the 3'- and 5'-ends of the sgRNA structure (**Table 2**). These modifications increase resistance to degradation by cellular nucleases, ensuring greater stability and enhanced performance throughout the gene editing process.

Table 2 Sequences of sgRNA scaffolds

[redacted]

[redacted]

5.1.2. Efficient ex vivo base editing in LCA16 patient-derived fibroblasts

To explore the specificity of ABE at the endogenous human *KCNJ13* locus within patient-specific cells, we delivered ABE8E mRNA and sgRNA into fibroblasts derived from an LCA16 (W53X homozygous) patient (Fibro$^{W53X/W53X}$). Five days post-treatment, base editing efficiency was assessed by deep sequencing (**Table 1**). As expected, the activity of ABE8E yielded efficient AT to GC editing (52.31 ± 0.06%) at the target W53X site (A^{6}). Cells from both the treated and untreated populations had low levels of other substitutions (or possibly sequencing error) in the amplicon, including bystander A>G and other T>G, T>C, G>A substitutions, with ABE8E exhibiting 6.48 ± 1.44% unwanted substitutions, and untreated Fibro$^{W53X/W53X}$ cells showing 2.56 ± 0.02% unwanted substitutions (**Figure 4** A). Rare indel outcomes were detected in the ABE8E-treated samples (2.71 ± 0.40%) (**Figure 4** A). Bystander A>G editing near the target nucleotide was rare in the ABE8E-treated samples (A^{14}; 0.26 ± 0.03%, A^{17}; 0.07 ± 0.07%) (**Figure 4** B). ABE activity upstream of the protospacer at positions A^{-2} (0.34 ± 0.025%) and A^{-9} (0.08 ± 0.08%) (**Figure 4** B) was also marked. This bystander editing within and outside the protospacer resulted in silent (L48L) and missense (D50G, M51V, M56V, M57V) mutations (**Figure 4** C), at a very low frequency (<1%) in Fibro$^{W53X/W53X}$.

Figure 4 On-target evaluation of ABE8E to correct the W53X allele in LCA16-patient fibroblasts

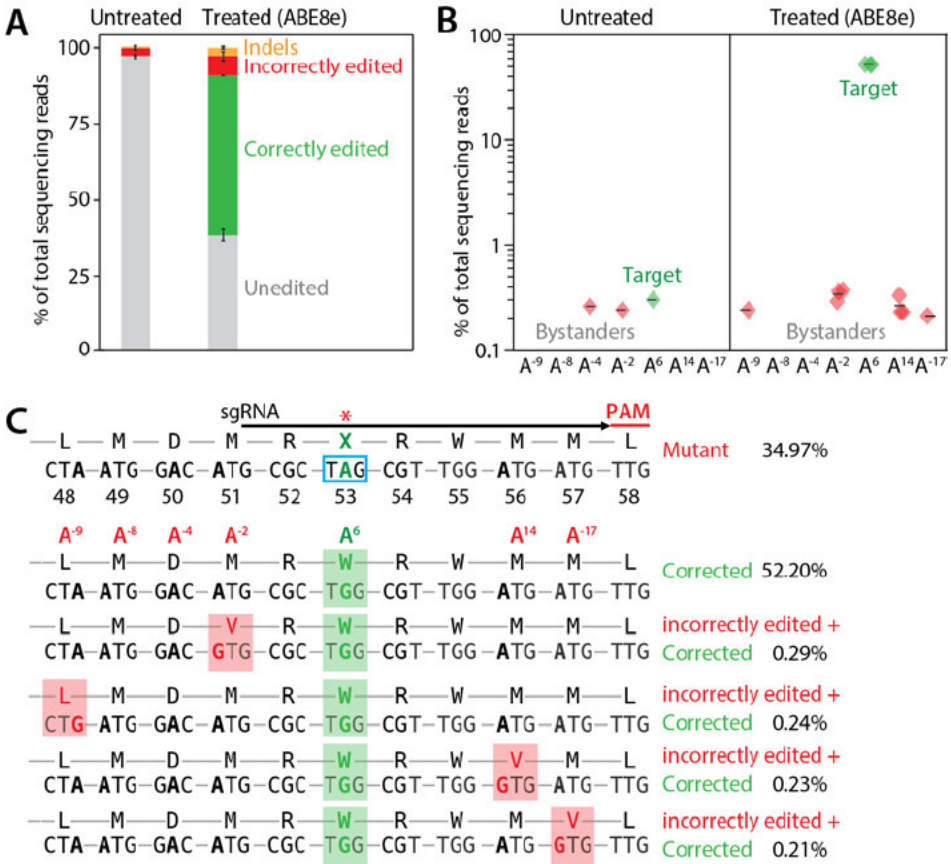

Legend: **(A)** Base editing efficiencies are shown as the % of total DNA sequencing reads, classified as unedited, correctly edited, incorrectly edited due to bystander 'A' edits, and with indels in treated and untreated (UT) cells. **(B)** % Editing of the target (A^{6}) and bystander (A^{-9}, - A^{-8}, A^{-4}, A^{-2}, A^{14}, A^{17}) 'A' to 'G' by ABE8E mRNA as observed in three independent experiments. **(C)** Amino acid conversion at the respective location was generated due to target and bystander edits. The protospacer sequence is underlined, the pathogenic early stop codon is in a purple box, the target 'A>G' edit is marked in

orange and bystander 'A' edits are in green. The sgRNA location is marked by a black line, PAM by a red line, and mutation in the blue box. All the 'A' bases within the protospacer are numbered 1-20 based on location. The 'A' bases downstream of the protospacer are numbered from -1 to -9, considering +1 as the first base of the protospacer. The top 10 most frequent alleles generated by ABE8E mRNA treatment show the nucleotide distribution around the cleavage site for sgRNA. Substitutions are highlighted in bold, insertions are shown in the red box, and dashes show deletions. The scatter plot shows the frequency of reads observed in treated cells (n=3 biological replicates). Figures presenting data from replicates are mean ± SEM.

Using the lead candidate with the protospacer and scaffold for targeting T153I in **Table 1** and **Table 2**, the specificity of ABE8E at the endogenous human T153I *KCNJ13* locus within patient-specific cells will be determined in a similar fashion by delivering ABE8E mRNA and sgRNA into fibroblasts derived from an LCA16 (T153I homozygous) patient[29] (Fibro$^{T153I/T153I}$).

[redacted]

Because the therapeutic effect is mediated through the DS, comprised of ABE8E mRNA and guide RNA, and not the delivery vehicle (LNP), we do not expect significant differences in DS function or mechanism of action whether delivered by SNC or UW-LNP-ABE8E. Here, we present the data collected using SNC to enable the discussion of the DS and cell-based assays. All data will be replicated using the intended [redacted] delivery, and the Sponsor is currently collecting data in these same models with this system.

[redacted]

Figure 5 Gene Editing *in vivo* After Delivery of the [redacted] LNP Formulation Used in UW-LNP-ABE8E

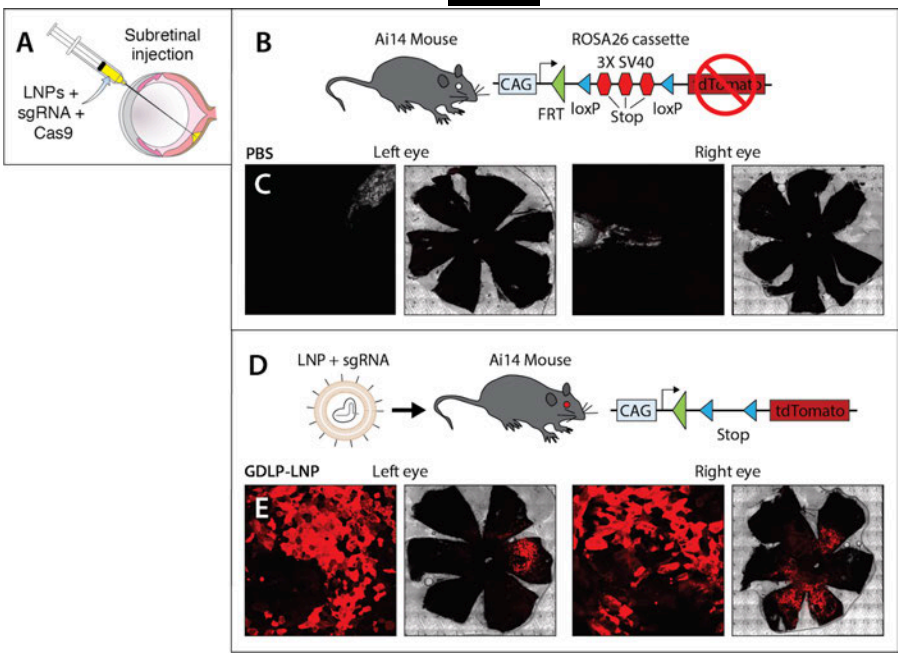

Legend: Using subretinal injection **(A)**, [redacted] LNPs were used to deliver sgRNA targeting the SV40 PolyA site of the Ai14 mice and Cas9-mRNA (1.5 ug dose; 1:4 sgRNA:Cas9 weight ratio). **(B-C)** Knock-in into *Rosa26* of a cassette with CAG-loxP-Stop-loxP- tdTomato in the Ai14 mice. (C) Injection of PBS has no tdTomato signal in the RPE. **(D-E)** Excision of the stop cassette after editing with sgRNA and Cas9-mRNA delivered using [redacted] LNPs, resulting in tdTomato expression. The expression of tdTomato (red) within the RPE floret fluorescence after 14 days confirms the successful delivery of the payload and editing of the RPE cells.

5.1.5. ABE8E mRNA corrects W53X in HEK^{W53X} cell model of LCA16

The Sponsor generated HEK cells that stably express GFP-tagged KCNJ13-W53X (HEK$^{W53X/W53X}$), and an isogenic WT control line, (HEK$^{WT/WT}$) in which the WT *KCNJ13* sequence was inserted into a single Flp-In recognition target (FRT) site at a transcriptionally active genomic locus (**Figure 6** A-B). We chose the ABE8E base editor due to its high efficiency and designed sgRNAs based on the predicted editing window at protospacer positions 4-8, counting PAM as position number 21-23. One of the three sgRNAs (G*C*G*CUAGCGUUGGAUGAUGU, PAM; TGG) was predicted to have high specificity while also placing the c158G>A position within the editing window of ABE8E (**Figure 6** B,D). We assessed the activity of ABE8E in mRNA and protein formulations via electroporation. HEK^{W53X} cells were electroporated with a mixture of ABE8E mRNA and sgRNA. Deep sequencing analysis was performed on the treated cells by isolating RNA instead of DNA to distinguish the inserted allele from the endogenous allele of the HEK genome. The pool of electroporated HEK^{W53X} cells showed significant AT to GC correction efficiency with ABE8E mRNA (53.02 ± 1.38%; **Figure 6** D-E).

The W53X nonsense mutation in *KCNJ13* disrupts its protein expression and trafficking in HEK^{W53X} cells, so whether base editing restored Kir7.1 expression and subcellular localization at the protein level was assessed. Immunocytochemistry demonstrated that the Kir7.1 protein is present in the membrane in most of the base-edited HEK^{W53X} cells, similar to control HEK^{WT} cells. The fluorescence signal in untreated HEK^{W53X} cells is accumulated in the cytoplasm and nucleus due to its premature truncation (**Figure 6**). These results confirmed the successful translation and trafficking of full-length protein after editing.

Figure 6 Evaluation of ABE8E to correct W53X *KCNJ13* allele in human cells

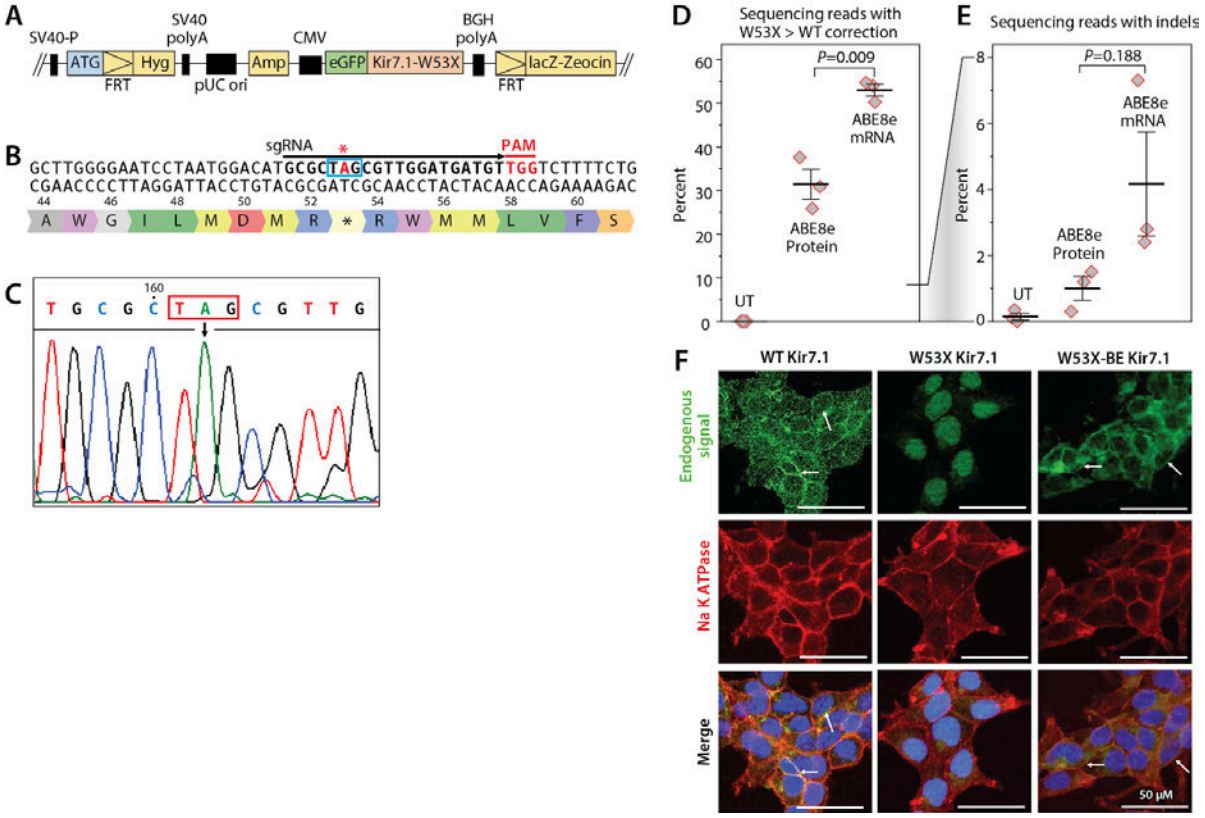

Legend: (A) Construct design to generate HEK293 FRT stable cells harboring the KCNJ13 ^{W53X} allele. **(B)** Schematic of the hKCNJ13 locus highlighting the mutation c.158G>A (blue box marked with *) and position of the W53X targeting sgRNA (black line) with TGG PAM (red line). **(C)** Chromatogram generated from HEK293 FRT stable cells showing the W53X codon marked in the red box and the downward black arrow indicating the specific nucleotide change (G>A). **(D)** Base editing efficiencies are shown as the percentage of sequencing reads with the corrected WT allele (and no other silent changes, bystander edits, or indels) in HEK293^{W53X} cells following electroporation of ABE8E protein + sgRNA (RNP) or ABE8E mRNA + sgRNA (n=3). Markers (diamonds) represent the individual biological replicates (n=3), and error bars represent SEM. **(E)** % of sequencing reads with indels in ABE8E RNP and ABE8E mRNA treated stable cells (n=3). Markers (diamonds) represent the individual biological replicates (n=3), and error bars represent SEM. **(F)** Kir7.1 expression in ABE8E mRNA treated cells assessed by immunocytochemistry. GFP primary antibody was used to enhance the endogenous signal. DAPI was used to stain the nucleus—scale bar, 50 µm. The white arrows mark the membrane localization in cells.

5.1.6. Functional Recovery in HEK^{W53X} cell model of LCA16

The Sponsor has developed an automated patch-clamp system to measure Kir7.1 channel function. Whole-cell currents were recorded using an automated patch-clamp system from pools of either base-edited HEK^{W53X} cells, untreated HEK^{W53X} mutant cells, or untreated HEK^{WT} cells (**Figure 7** A-C). HEK^{WT} cells exhibited an inwardly rectifying Kir7.1 current in 5 mM K^+ external physiologic solution. The inward current increased in response to external 140 mM Rb^+ (a known activator of the Kir7.1 channel) by at least 4.5-fold (**Figure 7**).

Figure 7 Automated patch-clamp recordings from ABE8E-edited human cells

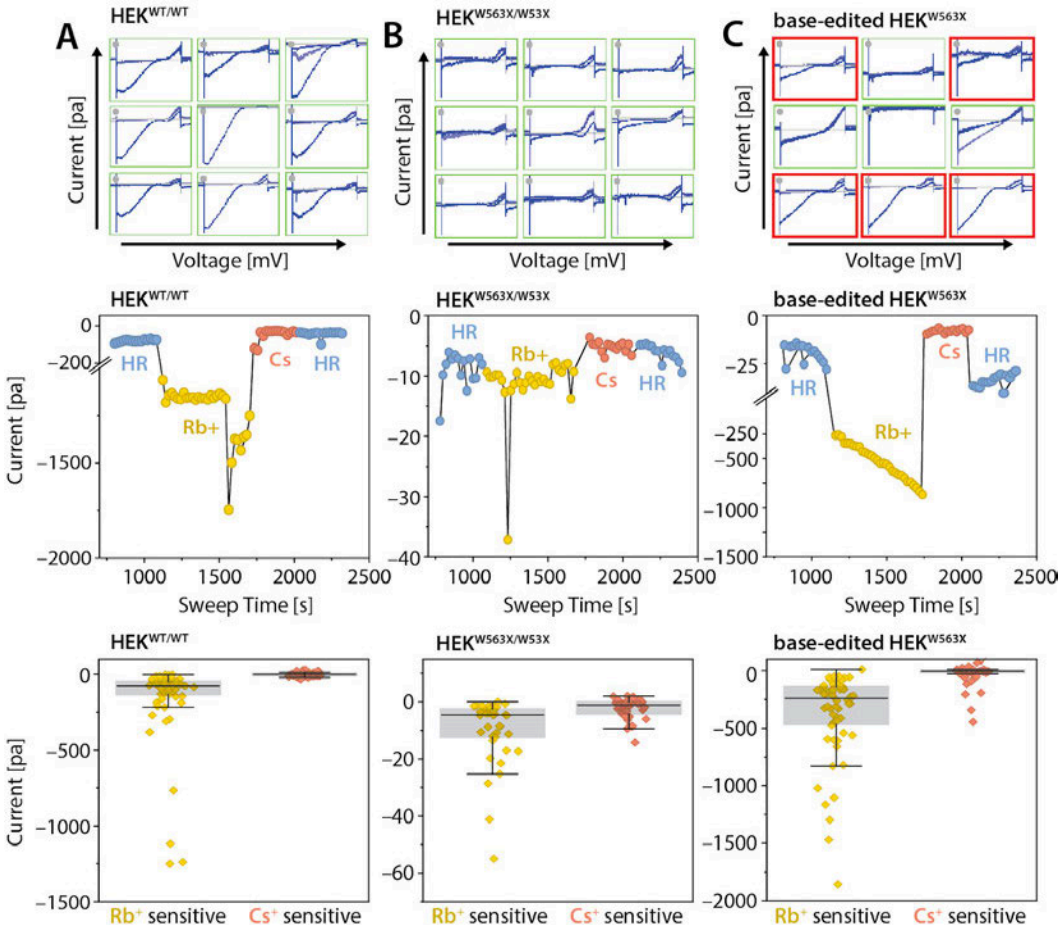

Legend: I-V curve and fold increase by Rb^+ for **(A)** HEK^{WT} cells (n=9) showing an increase in negative current, **(B)** HEK^{W53X}, and **(C)** base-edited HEK^{W53X} cells. The middle panel is the comparison of the time course of specific response to Rb+ or Cs+. In the lower panel are current measures in all the cells measured at -150 mV membrane potential showing an increased current for Rb+ and inhibition of current by Cs+. The y-axis scale for W53X is several fold less compared to the WT and base-edited HEK^{W53X} cells.

These responses were not observed in untreated HEK^{W53X} mutant cells, which demonstrated a significantly lower resting current amplitude and negligible change upon adding Rb^+ or Cs^+ (**Figure 7**). Importantly, base-edited HEK^{W53X} cells exhibited restored Kir7.1 current in 80% of individual cells (n=60), and the characteristic Rb^+-sensitive K^+ current. The K^+ current profile of 20% of the treated HEK^{W53X} cells (n=15) was comparable to mutant HEK^{W53X} untreated cells, which we attribute as unedited cells (**Figure 7** C) in the pool. From these experiments, we conclude that ABE8E mRNA + sgRNA delivery can correct the W53X mutation at high efficiency in vitro (around 50% of total alleles and in 80% of cells), restoring Kir7.1 protein levels and K+ conductance. The Sponsor intends to use the patch clamp assay as an important indicator to assess the efficacy of the intended DP. Importantly, these data show that the correction of errors in the *KCNJ13* gene restores K^+ conductance, reflecting the proposed mechanism of action to treat LCA16.

5.1.7. Off-target assays for nonviral base editor therapeutics

The Sponsor, in published work[26], has conducted off-target nomination *in silico* using Cas-OFFinder. This fast and versatile algorithm searches for potential off-target sites of Cas9 RNA-guided endonucleases in any sequenced genome rapidly without limiting the PAM sequence or the number of mismatched bases. The results of this assay are in **Figure 8**.

The Sponsor supplemented the bioinformatic nomination of off-target sites with an orthogonal empirical assay to identify the genomic sites that are at the highest risk for an unintended editing event. The Tsai lab, as collaborators within the SCGE, employed CHANGE-seq-BE (circularization for high-throughput analysis of nuclease genome-wide effects by sequencing), a scalable, automatable tagmentation-based method for measuring the genome-wide activity of Cas9 in vitro. CHANGE-seq-BE leverages a Tn5 tagmentation-based workflow to efficiently generate circularized genomic DNA libraries for defining the genome-wide activity of the genome editor. To assess off-target effects of sgRNA in a heterogeneous genomic background, we used iPSCs from three different donors to prepare genomic DNA libraries. One iPSC line was LCA16 patient-derived, harboring homozygous mutations in *KCNJ13*. The second line was from an unaffected family member (parent) of the LCA16 patient and contains a heterozygous mutation in *KCNJ13*. The third line was derived from iPSCs of another individual unrelated to the LCA16 patient, thus providing a good range of heterogeneity in genomic backgrounds for sgRNA off-target analysis. The results of these assays with three preparations of our sgRNA are summarized in **Figure 9**. The three preparations include different heavy internal chemical modifications to the sgRNA that could affect stability and specificity of the sgRNA in the patient, and also in the CHANGE-Seq-BE. The results of the CHANGE-Seq-BE using the intended DS show that the sgRNA and ABE8E used in UW-LNP-ABE8E have a clean profile (0.9 specificity score; **Figure 9**) with approximately 10 potential off-target sites with more than 10 reads, none of which are in an oncogene or other gene of concern. Additionally, all off-target effects are below 4% of the on-target result, and these are not expected to pose a concern for *in vivo* off-target editing especially with transient expression of ABE8E. These off-target sites will then be validated using rhAMP-seq in iPSC-derived RPE cells from patients and healthy donors to confirm the most common off-target edits that may occur using UW-LNP-ABE8E.

Figure 9 CHANGE-Seq-BE nomination of RUO grade sgRNA using W53X patient-derived iPSCs

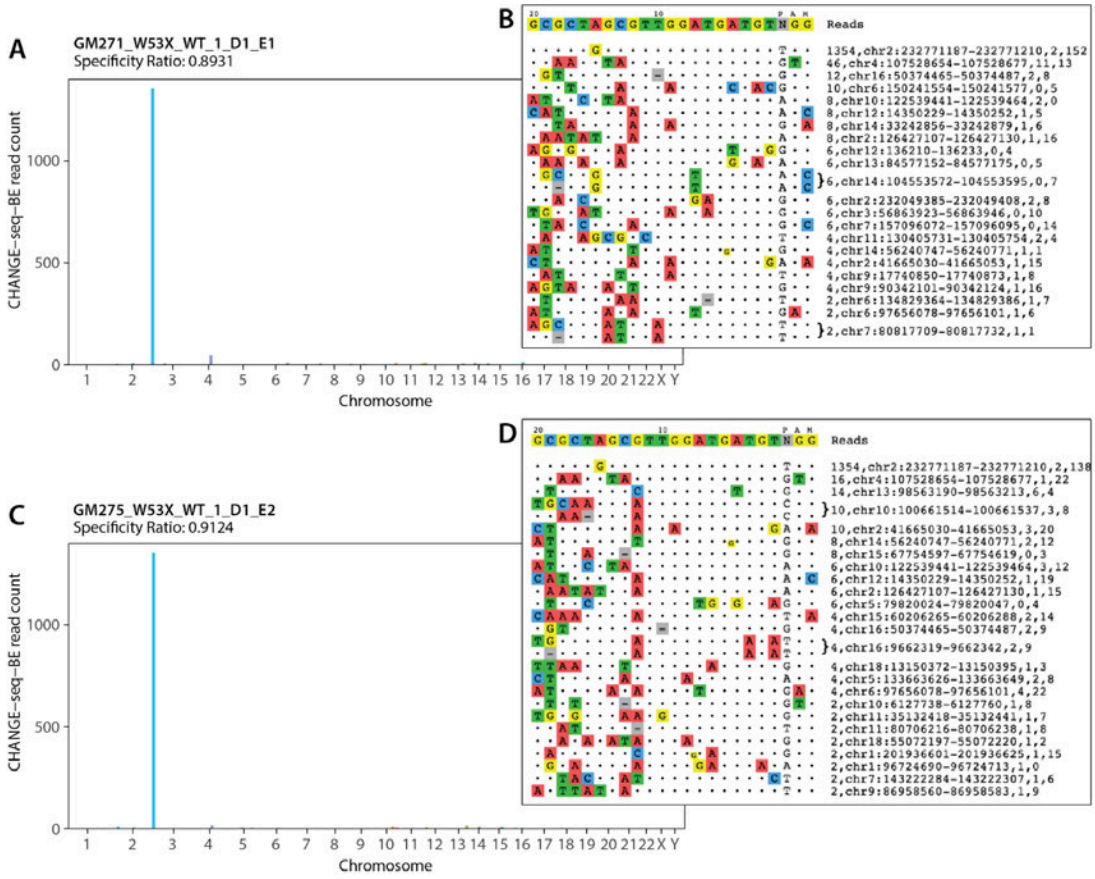

Legend: Read counts in CHANGE-Seq-BE assay from treatment of LCA16 patient-derived iPSC$^{W53X/W53X}$ with the ABE8E protein and the sgRNA within the DS. **(A-B)** First assay. **(C-D)** Second technical replicate. Nominated off-target sites detected by CHANGE-Seq-BE are organized by the number of read counts.The on-target site is the first line on the list.

Within LCA16 patient-derived cells treated with nonviral editors, we have verified the off-target activity of our editor at nine nominated off-target sites by performing rhAmp sequencing, a highly efficient RNase H2-dependent PCR technique that can amplify different targets using a single PCR reaction. The results of these assays are summarized in **Figure 10**.

Figure 10 Verification of on-/off-target activity at nominated sites in LCA16 patient-derived iPSC-RPE

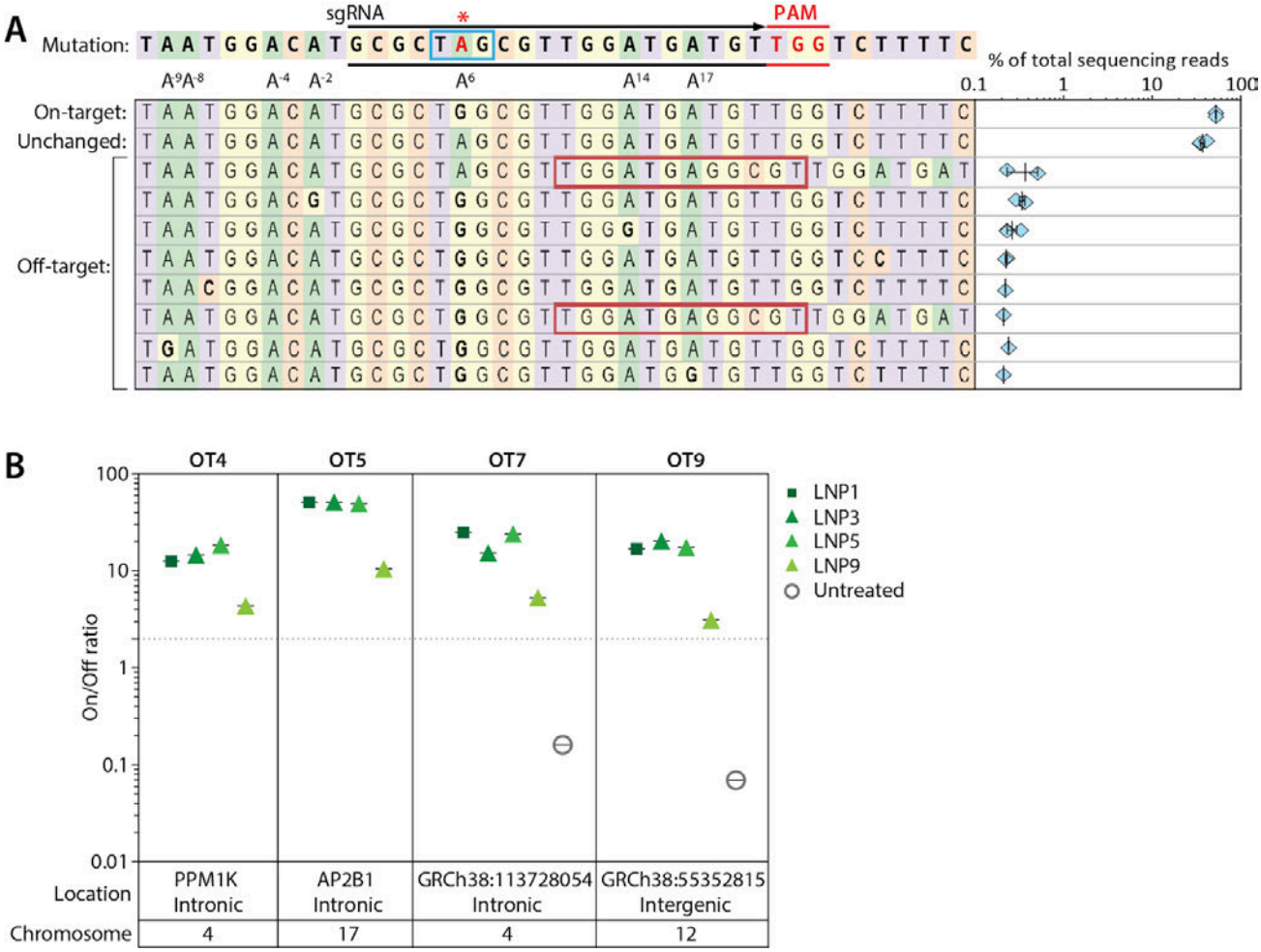

Legend: (A) The sgRNA location is marked by a black line, PAM is marked by a red line, and mutation is in the blue box. All the A bases within the protospacer are numbered 1-20 based on location. The A bases downstream of the protospacer numbered from -1 to -9, considering +1 as the first base of the protospacer. The top 10 most frequent alleles generated by ABE8E mRNA treatment show the nucleotide distribution around the cleavage site for sgRNA. Substitutions are highlighted in bold, insertions are shown in the red box, and dashes show deletions. The scatterplot shows the frequency of reads observed in treated cells (n=3 biological replicates). Data from replicates are represented as means and SEM. **(B)** On-target editing=A to G correction of pathogenic LCA-causing W53X allele of *KCNJ13.* Off-target modifications=indels and substitutions observed by next-generation sequencing (NGS) at the nominated off-target site. All nanoparticle formulations had >2 On/Off ratio for each of the nominated off-target sites (OT4, OT5, OT7, OT9). System: LCA16 patient-derived iPSC-RPE (W53X/W53X genotype treated with nanoparticles).

5.1.8. Patient-derived iPSC-RPE cell model of LCA16

The Sponsor has developed multiple cell-based assays to evaluate the ability of UW-LNP-ABE8E to make the corrective edit on *KCNJ13*. An induced pluripotent stem cell iPSC-RPE$^{W53X/W53X}$ model carrying a homozygous nonsense mutation in exon 2 of the *KCNJ13* gene (W53X) was generated from an LCA16 patient biopsy. Characterization of this LCA16 iPSC-RPE$^{W53X/W53X}$ model is consistent with cellular hallmarks of LCA16 disease, including a lack of Kir7.1 protein (**Figure 11** A-C), and a lack of inwardly rectifying K+ current (**Figure 11** D, E), similar to a Kir7.1-deficient mouse model and the HEK$^{W53X/W53X}$ cell line exogenously expressing the human W53X Kir7.1 variant described previously.[2,6] The Sponsor has also established a "wildtype" iPSC-RPE line with

cells obtained from fully correcting the W53X mutation in LCA16 patient iPSCs, which will be used as study controls.

The Sponsor has characterized the iPSC-RPE$^{W53X/W53X}$ cell line to demonstrate the link between W53X correction by base editing and Kir7.1 channel function to ensure the suitability of the patient-derived cells for use in a functional assay. Kir7.1 channel current (**Figure 11** D), cellular membrane potential (**Figure 11** E), and membrane localization (**Figure 11** F) were rescued by transducing this model with a lentiviral-mediated gene augmentation therapy comprised of DNA encoding full-length wildtype Kir7.1. In total, we have created an iPSC-derived cellular model and functional assays to measure Kir7.1 channel function and detect functional rescue after therapeutic delivery[7].

Figure 11. Functional rescue of patient-derived iPSC-RPE cell model of LCA16.

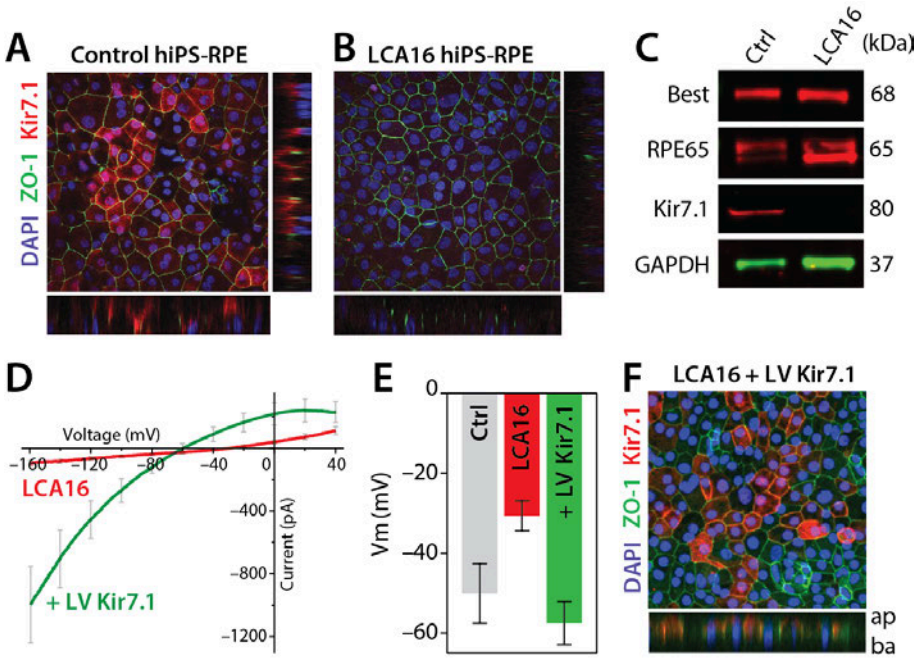

Legend: (A-C) Kir7.1 protein is not expressed in LCA16 iPSC-RPE. **(D, E)** Kir7.1 current and membrane potential rescue after gene therapy in LCA16 iPSC-RPE. **(F)** Protein localization to the membrane after gene therapy.

5.1.9. Rescue of Kir7.1 channel function in patient-derived iPSC-RPE$^{W53X/W53X}$

The Sponsor did not observe any toxicity in the ABE8E-treated iPSC-RPE$^{W53X/W53X}$, and cell morphology was comparable to untreated iPSC-RPE$^{W53X/W53X}$ (**Figure 12** A). Deep sequencing analysis in the base-edited iPSC-RPE$^{W53X/W53X}$ revealed 17.82 ± 1.53% editing of the mutant nucleotide to the wildtype sequence following ABE8E treatment (**Figure 12** B). Less than 4% of resultant alleles carried undesired genomic outcomes: indels quantified in treated RPE had a frequency of 0.68 ± 0.11% compared to 0.01 ± 0.002% in untreated controls, and bystander substitutions quantified in treated RPE totaled 2.94 ± 0.42% compared to 1.78 ± 0.07% in untreated controls (**Figure 12** C).

Manual patch-clamp electrophysiology was carried out on the pool of base-edited iPSC RPE$^{W53X/W53X}$ cells (**Figure 12** D) to assess the functional rescue of the Kir7.1 channel. Three types of Kir7.1 current profiles were observed in the edited iPSC-RPE$^{W53X/W53X}$ pool, classified into three groups: high-, medium-, and low-responding cells. Some of the cells (n=5 out of 13) showed a normal amplitude of K^+ current (-101.98 ± 0.07 pA) in physiological extracellular K+ solution, which was potentiated in Rb^+ external solution by 8-fold (-820.97 ± 265.54 pA). These high-responding cells showed a normal amplitude of K^+ current, rescue of Kir7.1 channel

function and were most likely to have only W53X>WT correction. Some of the cells did not show any recovery of Kir7.1 current and had a similar profile to iPSC RPE$^{W53X/W53X}$ cells[7]. These low-responding cells (n=4 out of 13) likely experienced no base editing. A few cells (n = 4 out of 13) showed slightly higher Rb^+-potentiated current than the untreated iPSC-RPE$^{W53X/W53X}$ cells, but not as high as iPSC-RPE$^{WT/WT}$ cells. The medium-responding cells showed a lower-amplitude Rb^+ response than the high-responding cells. We hypothesize that medium-responding cells contain a relatively low number of ion channels translated from a correctly base-edited *KCNJ13* allele. The current-sweep plots of the representative cell under different treatment solutions are shown in **Figure 12** E. In total, the Sponsor has created a patient-derived, iPSC-RPE$^{W53X/W53X}$ cell model that can be used to measure the gene correction and resulting functional improvement of cells treated with the intended DS. This confirms that the proposed mechanism of action for treating the W53X mutation by base editing results in the production of Kir7.1 channels and the restoration of wild-type function.

Figure 12 Evaluation of ABE8E to correct W53X alleles in iPSC-RPE$^{W53X/W53X}$

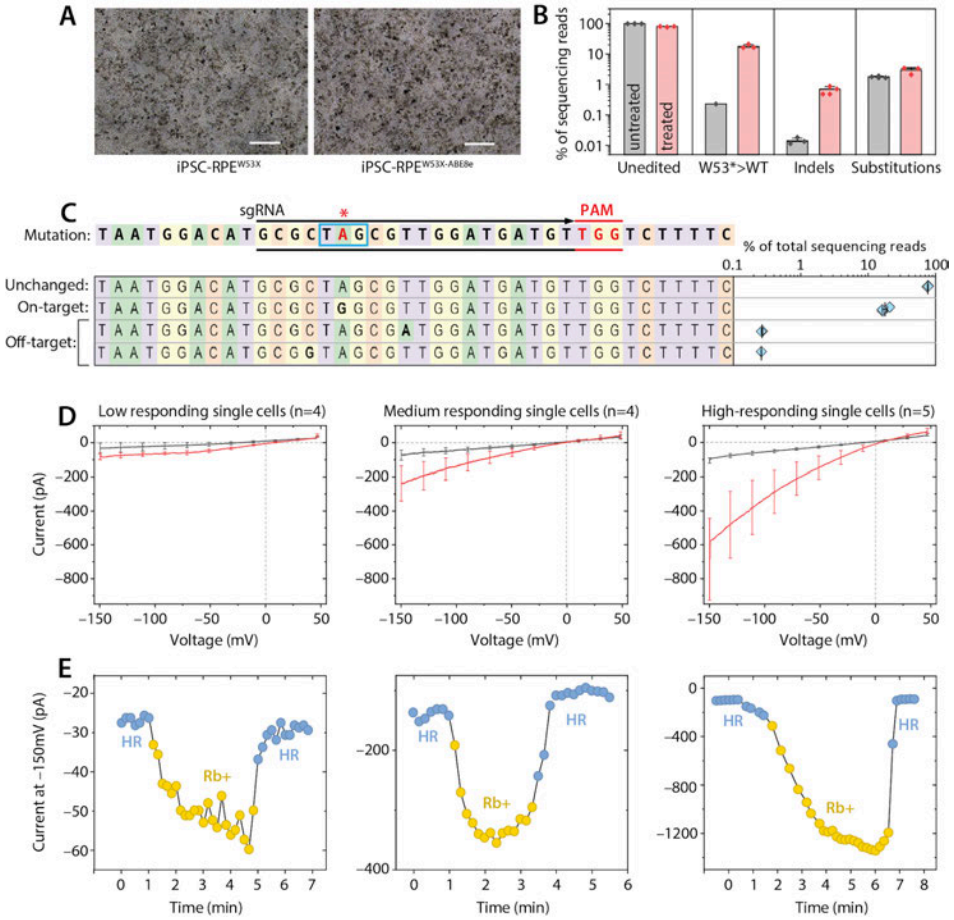

Legend: (A) Representative bright-field images of base editor treated and untreated iPSC-RPE$^{W53X/W53X}$. Scale bars = 100 µm. **(B)** Base editing efficiencies following treatment (BE) with ABE8E mRNA and sgRNA encapsulated in SNC-PEG nanoparticles in iPSC- RPE$^{W53X/W53X}$ as compared to untreated (UT) cells. Reads from the UT and treated cells (n=3) were categorized into 4 subtypes based on their sequences, unedited, W53X>WT, indels, and substitutions. **(C)** Reads generated by ABE8E mRNA treatment showing the nucleotide distribution around the cleavage site for sgRNA. Substitutions are highlighted in bold. The scatter plot shows the frequency of alleles observed in treated cells (n=3). Lines and error bars are represented as mean ± SEM. **(D)** Manual single-cell patch-clamp assays on iPSC-RPE^{W53X} cells after treatment with ABE8E. Of the 13 cells assessed for Kir7.1 activity, each could be binned into one of 3 classes: low-responding single cells, which appeared to be unedited mutant cells; medium-responding single cells, which showed a low level of Rb^+ response; and high-responding single cells, which showed Rb^+ response like iPSC-RPE^{WT} cells. The number (n) of cells binned into each

class is shown at the top of each graph. **(E)** Current-sweep plot from a representative cell of each bin across a time course of being exposed to physiological HR solution (gray), Rb^+ stimulation (red), and subsequent wash with HR solution (green).

5.1.10. *Kcnj13*$^{W53X/+}$ monoallelic knock-in mouse: an LCA16 model

The Sponsor has generated a mouse model to test the efficacy of UW-LNP-ABE8E at *KCNJ13*^{W53X} gene correction in a preclinical model. To test base editing efficiency *in vivo*, we created mice carrying a W53X substitution in the *Kcnj13* gene using CRISPR-Cas9 genome editing. In the pronuclei of zygotes, a combination of Cas9 protein, two different specific guides to the *Kcnj13* locus (GAATCCTAATGGACATGCGCTGG and TAATGGACATGCGCTGGCGCTGG), and ssODN was injected (**Figure 13** A-B). Five of six newborn mice genotyped by sequencing had only one allele with the nucleotide alteration, validated by restriction fragment length polymorphism (RFLP). The PCR product was digested with the NheI enzyme, which selectively digests the mutant allele (**Figure 13** C). Breeding of heterozygous founders resulted in homozygous mice and postnatal day one lethality[2,34] and was confirmed by genotyping (**Figure 13** D). Newly generated heterozygous mice displayed identical retinal phenotype to age-matched wildtype mice, measured by optical coherence tomography (OCT, **Figure 13** E). Electrical activity generated by the retina was recorded using full-field electroretinogram (ERG) as a measure of retinal function in response to a light stimulus. Specific retinal cells generate varying waveforms: a-, b- and c-wave. The a-wave, a negative deflection, corresponds to the photoreceptor. The b-wave, which is positive, arises from the inner retinal cells, while the c-wave is generated by the RPE cell. ERG evaluation of heterozygous mice was identical to that of wildtype mice. (**Figure 13** F).

There is no mouse model harboring a homozygous pathogenic mutation in the *Kcnj13* gene. We have determined that unlike in humans, at least one wildtype *Kcnj13* allele is required for survival beyond postnatal day 1[2,34]. Therefore, we used our *Kcnj13*$^{W53X/+}$ mice to generate an LCA16 mouse model (*Kcnj13*$^{W53X/+\Delta R}$) using a Cas9 nuclease complex targeted to disrupt the wildtype allele (**Figure 13** A-B). The wildtype allele was disrupted in the RPE cells by delivering Cas9 mRNA and sgRNA through sub-retinal delivery, using SNC as a delivery vehicle. Mice were evaluated after 6 weeks to demonstrate intact retinal structure (**Figure 13** E, lower panel). ERG measurements of c-wave amplitude before the injection was decreased by 54%, which reflects the functional loss of RPE cells as in LCA16. In total, the Sponsor has developed a mouse model for replicating LCA16 caused by *KCNJ13*^{W53X} mutation that will serve as the nonclinical animal model for evaluating UW-LNP-ABE8E efficacy.

Figure 13 Visual function of *Kcnj13*$^{W53X/+}$ mice is similar to *Kcnj13*$^{+/+}$ mice

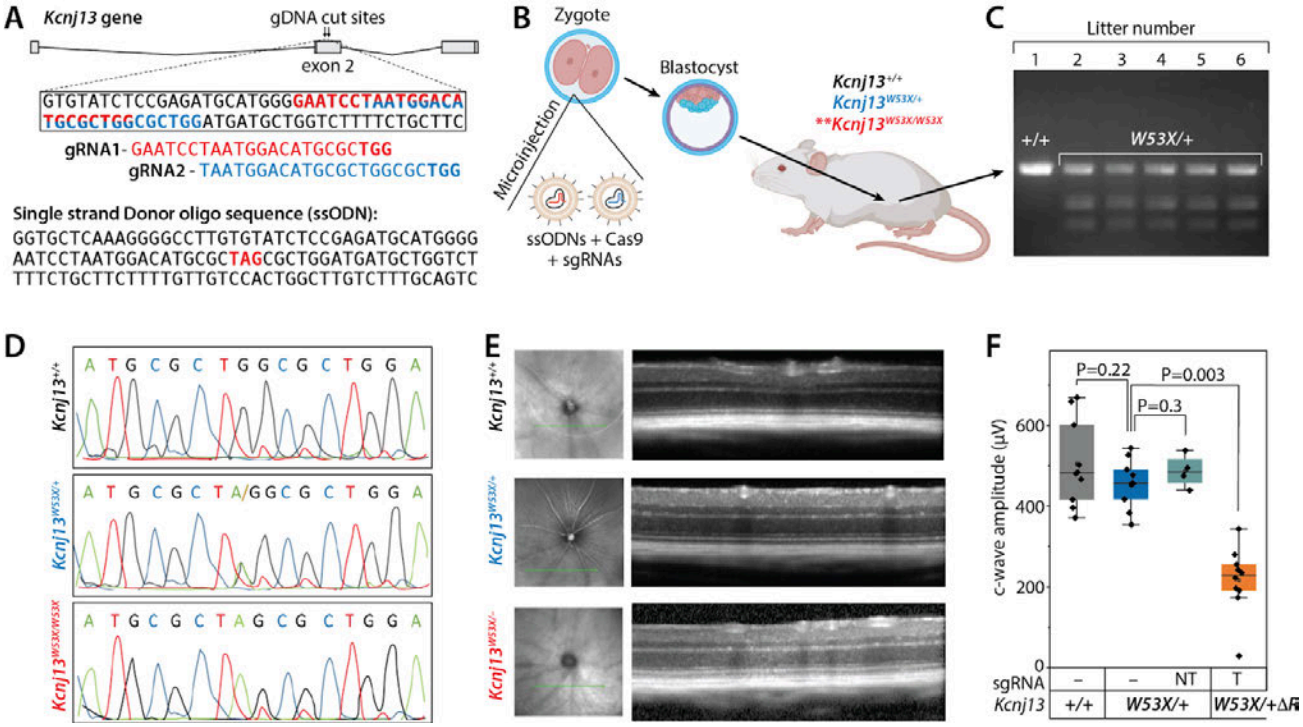

Legend: (A) Two different sgRNA targeting the *Kcnj13* gene at exon 2 and a ssODN sequence with the desired nucleotide change to generate the *Kcnj13*$^{W53X/W53X}$ **(B)** mouse model by CRISPR/Cas9 and HDR genome editing technique by microinjecting them into the pronuclei of the zygote. **(C)** RFLP analysis of the *Kcnj13* gene from the newly generated mice digested with Nhe1 enzyme on 2% agarose gel. **(D)** Chromatograph confirming the mouse genotype. **(E)** OCT images showing the comparison between *Kcnj13*$^{+/+}$, *Kcnj13*$^{W53X/+}$, and WT allele-disrupted *Kcnj13*$^{W53X/+\Delta R}$ mice. **(F)** Averaged c-wave response confirming WT allele disruption in the RPE of *Kcnj13*$^{W53X/+\Delta R}$ using the targeted guide (T). (**= postnatal day1 lethal; NT= not targeting sgRNA)

5.1.11. In vivo base editing via subretinal injection of ABE8E

Because the *Kcnj13* gene is not wholly conserved between humans and mice, the Sponsor created sgRNAs targeting the W53X allele (**Figure 14** A) of mouse *Kcnj13*, which was validated in the fibroblasts derived from *Kcnj13*$^{W53X/+}$ mice via electroporation (**Figure 14** B). For *in vivo* subretinal delivery into *Kcnj13*$^{W53X/+}$ mice, ABE8E mRNA, sgRNA, and GFP mRNA were delivered via subretinal injection. The injection site could be located through GFP fluorescence (**Figure 14** C), GFP-positive RPE tissue, and the choroid optic cup were dissected for deep sequencing of the *Kcnj13* locus. ABE8E mRNA and sgRNA delivery resulted in RPE editing at two different doses (n=4 eyes for each dose) (**Figure 14** D). A dose range finding (DRF) study will be conducted to determine the optimal dose of ABE8e mRNA/eye. On-target analysis showed no other A>G substitutions outside or within the protospacer region, and indel mutations were not significantly increased over placebo-treated mice (**Figure 14** E). These data demonstrated the specific editing of the W53X allele in vivo by ABE8E.

5.1.12. Base editing of the LCA16 mutant allele improves RPE function

The Sponsor conducted proof-of-concept studies in *Kcnj13*$^{W53X/+\Delta R}$ mice by editing the mutant allele via subretinal administration of the ABE8E mRNA and specific guide packaged in SNC. ERG measurements were performed at weeks 2, 6, and 10 to monitor longitudinal rescue in phenotype (**Figure 14** F). At week 10, mfERG was performed on injected eyes to determine if functional recovery was regionalized based on localized delivery of the base editor complex. For the control group, *Kcnj13*$^{W53X/+\Delta R}$ was injected with a ABE8E and a non-targeting guide.

The base-edited eyes showed an increase in the c-wave amplitude at all measured time points (**Figure 14** G-J) when compared with mice that were injected with ABE8E mRNA and a non-targeted guide. mfERG showed localized waveforms (**Figure 14** H) that may correlate with the site of injection (**Figure 14** C). At ten weeks post-injection, the normalized c-wave amplitude was increased for the targeted guide-delivered retina, and reduced for the retinas treated with non-targeted guides, while maintaining intact retinal structure as evaluated by OCT (**Figure 14** G-K). These results are proof-of-concept that suggest base editing of the *KCNJ13*^{W53X} allele restores retinal function and may be a viable treatment for inherited LCA16.

Figure 14 Phenotypic reversal of *Kcnj13*^{W53X} mice following *in vivo* ABE8E treatment

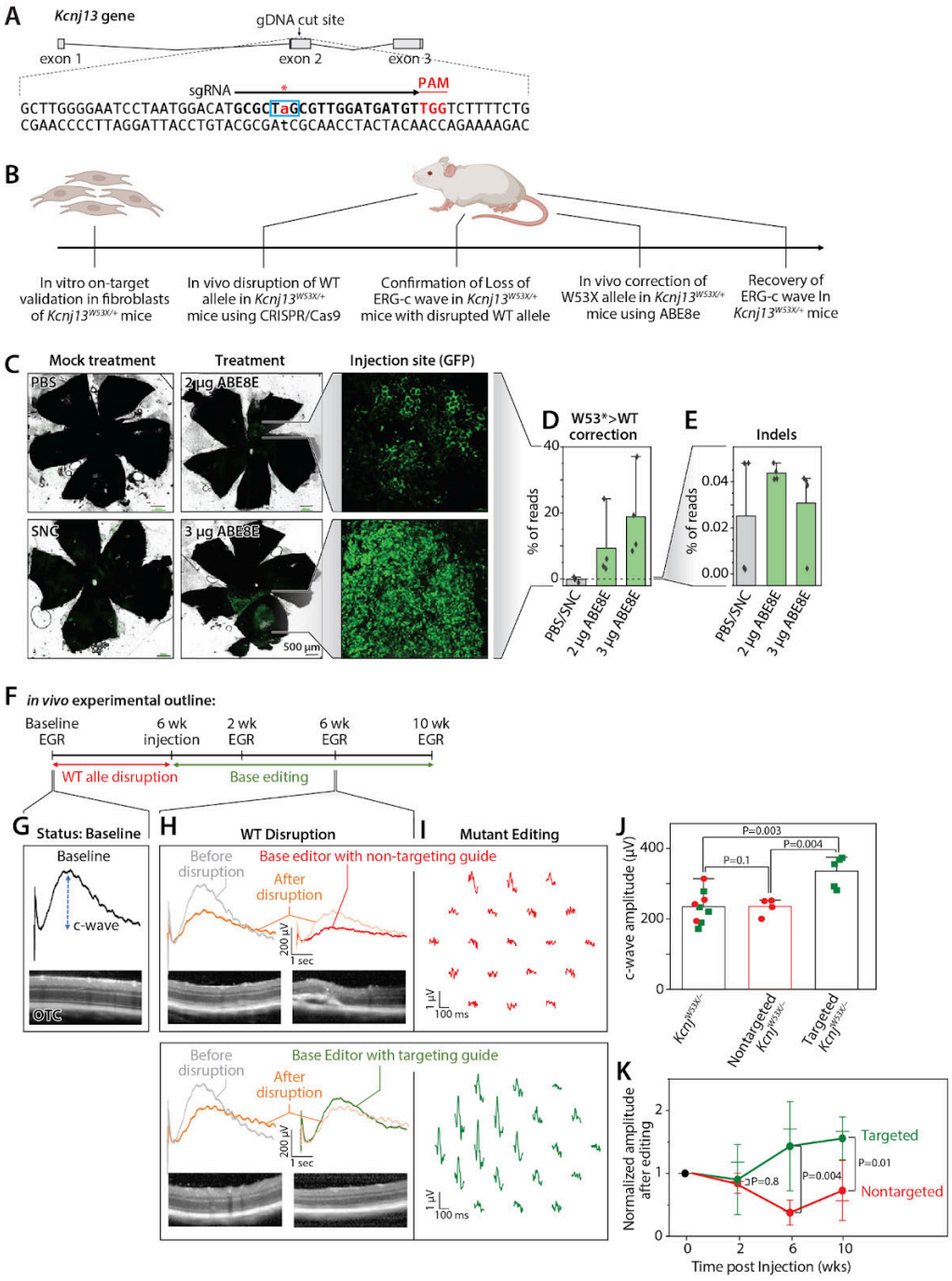

Legend: (A) The sgRNA design targeting the *Kcnj13*^{W53X} allele for base editing, with the black arrow representing the sgRNA spacer sequence, the desired base editing site indicated by an asterisk, and the PAM shown in yellow. **(B)** Workflow of in vivo base editing strategy. **(C)** RPE floret of eyes subretinally injected with SNC-PEG-ATRA packaged ABE8E mRNA, W53X-sgRNA, and GFP mRNA or empty SNC-PEG-ATRA/PBS as a mock treatment. **(D)** % of cells with W53X>WT corrections, observed in *Kcnj13*$^{W53X/-}$ mice treated with 2 μg or 3 μg of ABE8E. **(E)** % of sequencing reads showing the indels, observed in *Kcnj13*$^{W53X/-}$ mice treated with 2 μg or 3 μg of ABE8E. **(F)** A timeline outlining the in vivo experiment. Baseline ERG is performed prior to the disruption of the WT allele and is followed up after 6 weeks. ERG is performed on mice prior to injection of the base editor, and recovery is monitored for 10 weeks**. (G)** Representation of the c-wave amplitude acquired from the *Kcnj13*$^{W53X/+}$ mice with the OCT image of the retina. **(H)** The reduction in c-wave amplitude of the *Kcnj13*$^{W53X/+}$ mice at 6 weeks after disrupting the wildtype allele with Cas9 protein and sgRNA guide specific to the wildtype allele. **(I)** c-wave traces and mfERG response following the injection of base editor with a non-targeting guide to the mutant allele (red) and base editor with a targeting guide (green). The faded traces are for comparison before the disruption of the WT allele (gray) and injection of the base editor (orange). **(J)** Bar graph comparing the c-wave amplitude 6 weeks after the disruption of the wildtype allele (blue) to the c-wave amplitude 6 weeks after the injection of base editor with a non-targeting guide (red) and targeting guide (green). **(K)** Normalized c-wave amplitude comparison between the eyes injected with non-targeting and targeting guides at weeks 2, 6, and 10. (ns= not significant).

5.1.13. Reporter Assay to Assess On-Target Editing

5.1.13.1. Design of initial proof-of-concept W53X reporter construct

A novel cell-based assay is in development which will serve as a quality control measure following the production of UW-LNP-ABE8E. A proof-of-concept fluorescence bicistronic expression construct was designed that contains cytomegalovirus (CMV) promoter driven mRFP and CMV promoter driven eGFP. The design is based upon prior base editor reporter strategies in human cells.[35,36] The *KCNJ13* W53X premature stop codon mutation site (GCTTGGGGAATCCTAATGGACATGCGCTaGCGTTGGATGATGTTGGTCTTTTCTG) was cloned upstream of and in-frame with mRFP, thereby inhibiting the expression of the mRFP reporter. Downstream of mRFP is CMV-driven eGFP which is designed to be unaffected by the W53X mutation. This construct was packaged in a lentivirus to transduce human HepG2 cells. Transduced cells were expanded in culture and sorted for GFP expression, confirming the establishment of a HepG2^{W53X} reporter cell line. Treatment of the cell line with UW-LNP-ABE8E should result in corrective adenine to guanine editing, thereby replacing the disruptive stop codon with tryptophan. This corrective editing results in successful translation through the mutation site, leading to the expression of mRFP and confirmation of successful on-target adenine base editing by UW-LNP-ABE8E. The design of the construct, LV-W53X-mRFP and experimental data is shown in **Figure 15**.

5.1.13.2. Proof of Concept for novel rapid reporter assay

To provide proof-of-concept data for the novel on-target reporter assay, HepG2 cells were transduced with the W53X construct described below (**Figure 15** A) and sorted for eGFP expression to create a HepG2^{W53X} cell line. Before treatment with UW-LNP-ABE8E, GFP^{+}/mRFP^{-} HepG2^{W53X} cells were observed. Three days after treatment with UW-LNP-ABE8E, mRFP was observed in the treated HepG2^{W53X} cells. This increase in mRFP expression was confirmed by flow cytometry at 3 days post-delivery (**Figure 15** C-E).

Figure 15 Proof-of-concept reporter cell line to report on-target editing

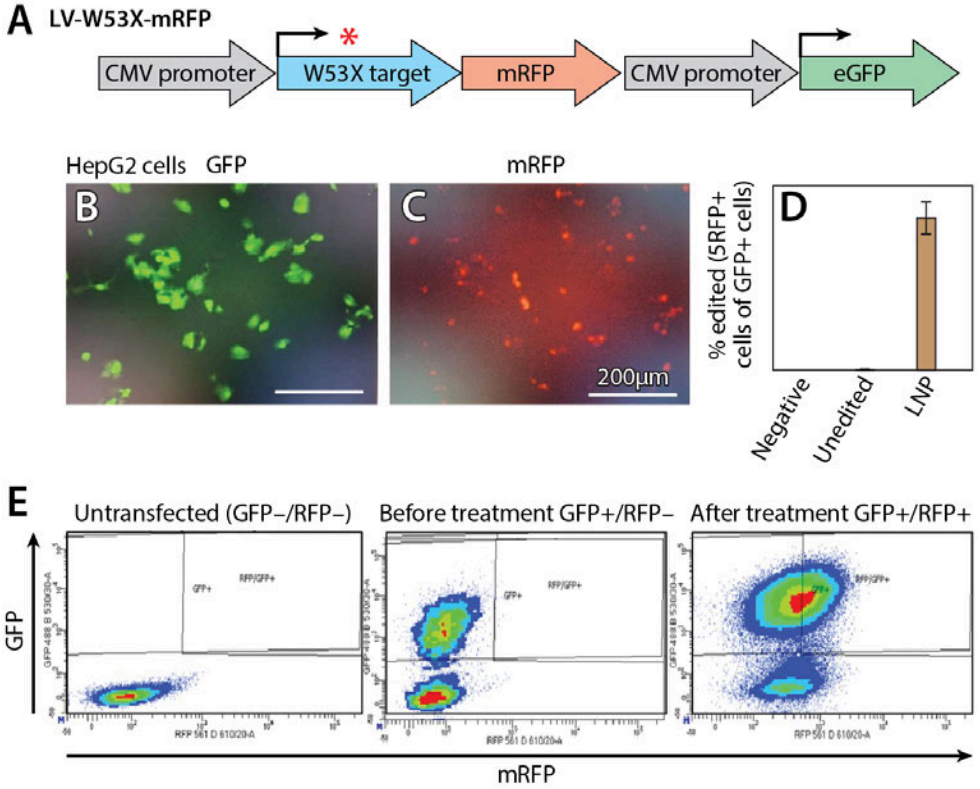

Legend: (A) Design of the lentiviral (LV) construct to generate the proof-of-concept HepG2^{W53X} reporter cell line. **(B)** HepG2 cells were transduced with the reporter construct and expressed GFP before treatment with UW-LNP-ABE8E. **(C)** mRFP is expressed after treatment with UW-LNP-ABE8E and on-target editing (scale bar represents 200 µm). **(D)** The population of mRFP^{+} cells increases after UW-LNP-ABE8E treatment (3 days post-treatment). **(E)** Representative flow cytometry showing untransfected cells (GFP^{-}/RFP^{-}; left), and reporter cells before treatment with UW-LNP-ABE8E (GFP^{+}/RFP^{-}; center), and reporter cells after treatment with UW-LNP-ABE8E (GFP^{+}/RFP^{+}; right).

5.1.13.3. Stable reporter cell line development

Upon passaging, the HepG2^{W53X} reporter cell line lost expression of the transgene after weeks in culture. To address this issue, a new construct was generated, replacing the poly-glycine linker with T2A (a self-cleaving protein). This new knock-in construct is designed to use defined CRISPR-based integration into the *AAVS1* locus via homology directed repair (HDR) to generate a stable cell line with durable expression of the reporter. This construct was electroporated in human HEK293 cells along with *AAVS1* guide and Cas9 ribonucleoprotein to develop this reporter line and qualify by assessing their efficiency in editing the W53X mutation. In early proof-of-concept experiments, HEK293 cells electroporated with this construct, *AAVS1* guide, and Cas9 express the expected protein (eGFP+/mRFP-) (**Figure 16** C). Development of this cell line is ongoing, with the goal of using it for further assessment of UW-LNP-ABE8E.

Figure 16 Design of reporter cell line to assess the on-target editing

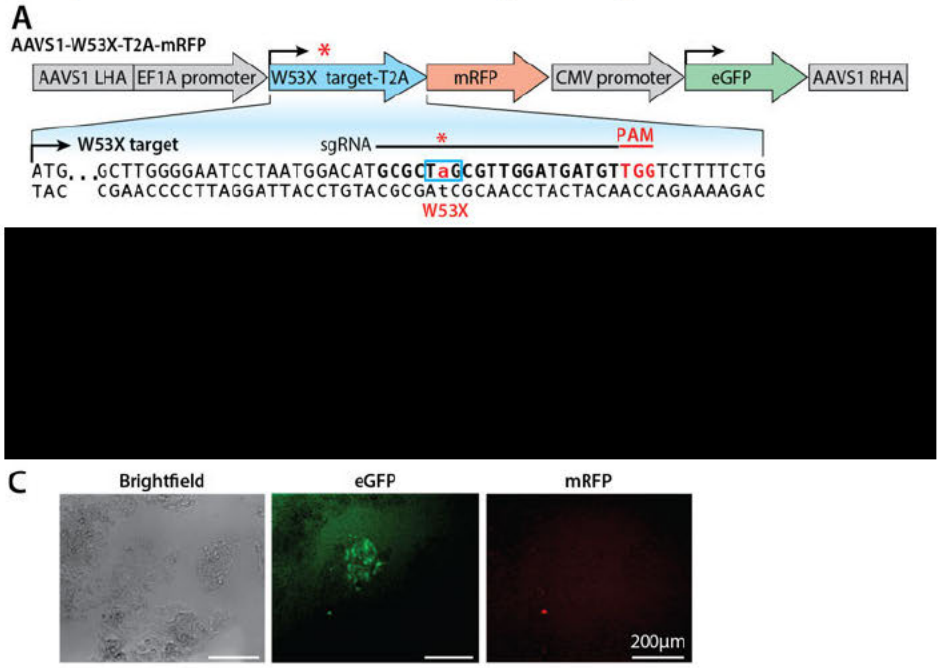

Legend: (A) AAVS1-W53X-T2A-mRFP, a novel construct to be used in the development of a stable, reporter cell line to assess the on-target editing ability of UW-LNP-ABE8E. **(B)** AAVS1-T153I-T2A-mRFP, similar construct for T153I. **(C)** Cells after electroporation of the cells without treatment with LNPs in brightfield (left) green (center) and red (right) channels. Electroporated cells express eGFP but not mRFP, as designed (scale bar: 200 µm).

To generate a reporter line for the T153I mutation, we will clone the T153I target site into a construct similar to the one for W53X (**Figure 16** B). The T153I mutation on the complementary strand to the A-base (C>T, where T is the mutant base paired with the A-base target of ABE8E) can be used to generate a TAG stop codon into the reading frame of the transcript for the reporter. Our ATG upstream of the target site shifts the reading so that the tAG stop codon terminates translation and therefore no mRFP or red fluorescence will be seen until the tAG in the reporter construct is edited. After ABE8E activity in the DP, editing of the T153I A on the complementary strand (which pairs with the T on the top strand) will generate a G. The TAG stop codon in the transcript will then be altered to CAG. This CAG codon for a glutamine would allow for full length transcription to proceed through to mRFP, to produce the same red fluorescent signal as seen in the proof-of-concept W53X experiments (**Figure 15 C**) Development of this T153I reporter cell line is ongoing, with the goal of using it for further assessment of UW-LNP-ABE8E-T153I.

Further, we will use long-read sequencing with Oxford Nanopore Technologies (ONT) to verify the integration site after HDR. The cell line verification of the reporter lines will be performed through short tandem repeat (STR) sequencing. STR profiling will be conducted on frozen cell pellet samples using the Promega PowerPlex 16HS system to analyze STR profiles and detect STR polymorphisms across 15 loci plus amelogenin. The strategy should detect cell-line cross-contamination at levels as low as 2-5%.

This reporter assay is intended to serve as a lot release test and may also be used for stability evaluation and comparability studies. As the UW-LNP-ABE8E manufacturing process is refined, a matrix of product characterization testing shall identify CQAs and CPPs with a goal of establishing a relationship between the test article's MoA and potency-related CQAs. As the program matures, in-process and lot release testing will be included to round out a robust potency assurance strategy. The goal of ongoing potency assay development is to qualify an assay that is specific and ensures that every lot of released DP will have the potency necessary to achieve the intended therapeutic effect.

5.1.14. Functional Restoration and Dose Range Finding (DRF) in W53X Mice

The Sponsor will conduct a dose-escalation study using research-grade UW-LNP-ABE8E via subretinal injection in 12 W53X mice (6 male, 6 female) (**Table 3**).

Table 3 Proposed nonclinical animal studies to assess UW-LNP-ABE8E

	Study	Animal Model	Sample size, *n*	Material Grade	Laboratory
1	Dose Range Finding	Mouse W53X	12 (6 male, 6 female)	RUO	R&D
2	Biodistribution	Mouse W53X	12 (Additional endpoints from study 1)	RUO	R&D
3	Pharmacology/Toxicology	NHP	6 (3 male, 3 female)	RUO	R&D
4	Definitive Safety/Biodistribution	Sprague-Dawley rat	36 (18 male, 18 female)	Engineering-grade or cGMP	GLP
5	Definitive Safety/Biodistribution	NHP	2 (1 male, 1 female)	Engineering-grade or cGMP	GLP

In preliminary studies, 0.5 - 1.5 µg of DS (sgRNA and ABE8E mRNA) have been delivered per eye. In the dose range finding (DRF) study, we will deliver 2, 3, 4, and 5 µg of DS. 5 µg of DS RNA is the upper dosing limit with the 2 µL injection volume. We will include two control groups: one at 4 µg DS/eye with non-targeting sgRNA and the other with vehicle injection. OCT, visual acuity, and ERG will be performed pre-injection and post-injection. During the post-injection period, ERG will be followed biweekly for 12 weeks. At the termination of the experiment, the tissue will be harvested for tissue morphology, Kir7.1 expression and protein production. We will evaluate the performance of these UW-LNP-ABE8E doses compared to scrambled and sham injections consisting of equal volume of buffer without LNPs. Specifications are shown in **Table 4** that would be met to demonstrate editing of W53X with the recovery of ERG a-, b-, and c-wave amplitudes, including: (1) the retina structure must appear normal, (2) full-length Kir7.1 protein must be expressed in the RPE cells. We will also determine immune-related gene expression by RT-qPCR, such as TNF-α transcript levels that indicate adaptive immune responses.

Table 4 Success criteria for the *in vivo* murine efficacy and safety studies

Performance characteristic	Measurement	Assay	Specifications in W53X het mice (efficacy and safety)
In vivo on-target outcome	W53X gene correction	NGS	>15% tAg > tGg editing
	Kir7.1 expression	IHC	Detectable Kir7.1 protein with RPE cell markers proximal to injection bleb
In vivo off-target outcomes	Editing at off-target DNA sites	NGS	<1% base edits and indels at top 10 off-target sites within RPE cells proximal to injection bleb
Behavioral	Visual function	ERG	Measurable (>100 µV) peak between 1-2 secs for c-wave relative to placebo UW-LNP-ABE8E
	Behavioral outcome	Survival	No change relative to non-targeted UW-LNP-ABE8E
Toxicology	White and red blood cells	Blood cell count	Within normal range for UW-LNP-ABE8E
	ALT, AST, GGT, AP, BUN, creatinine	Serum blood chemistry	Within normal range for UW-LNP-ABE8E
Antibody-mediated immune responses	Cas9 NAb titers	ELISA	Not detectable for UW-LNP-ABE8E

Cell-mediated immune responses	Number of CD4 and CD8 cells in vitreous and blood	IHC	Not detectable for UW-LNP-ABE8E
	Number of Cas9 reactive IFN-γ-secreting cells in vitreous and PBMCs	IFN-γ-ELISpot assay	Not detectable for UW-LNP-ABE8E

Legend: All specifications are relative to UW-LNP-ABE8E encapsulating a non-targeting sgRNA, unless otherwise indicated. ELISA: enzyme linked immunosorbent assay; ERG: electroretinogram; IFN: interferon; IHC: immunohistochemistry; NGS: next-generation sequencing; NAb: neutralizing antibody.

5.1.15. Other Biodistribution Studies

Additional endpoints in the mouse studies described above will be included to address the biodistribution of UW-LNP-ABE8E and all of its components to systemic tissues. Specifically, the ABE8E mRNA, sgRNA, [redacted] will be analyzed in blood and tissues including heart, lung, liver, kidney, and CNS. Gonads of male and female mice will be collected and analyzed for evidence of on-target and off-target editing as well as presence of all components of the DP.

5.1.16. Non-GLP Toxicity and Biodistribution in NHP using research-grade UW-LNP-ABE8E

The Sponsor will conduct preliminary safety/toxicity studies in NHP using research-grade materials to help define the later IND-enabling studies that will be conducted in a GLP-setting. Inflammation and potential toxicity will be monitored using retina imaging and ERG, followed by immunogenicity studies in 6 animals (3 males and 3 females; this is a typical pharmaceutical industry standard number of NHPs for toxicity regulatory studies in the extensive experience of Dr. Nork[8–11,37]), resulting in a total of 12 eyes treated with different doses of research-grade UW-LNP-ABE8E or equivalent experimental control (vehicle injection; 2 eyes).

Table 5 Success criteria for the *in vivo* NHP safety studies

Performance characteristic	Measurement	Assay	Specifications in NHP (efficacy and safety)
Behavioral	Visual Function	ERG	No change relative to sham vehicle control
	Behavioral outcome	Survival	No change relative to sham vehicle control
Inflammation	Retina pathology	IHC	No change relative to sham vehicle control
Toxicology	White and red blood cells	Blood cell count	Within normal range for UW-LNP-ABE8E
	ALT, AST, GGT, AP, BUN, creatinine	Serum blood chemistry	Within normal range for UW-LNP-ABE8E
Antibody-mediated immune responses	Cas9 NAb titers	ELISA	Not detectable for UW-LNP-ABE8E
Cell-mediated immune responses	Number of CD4 and CD8 cells in vitreous and blood	IHC	Not detectable for UW-LNP-ABE8E
	Number of Cas9 reactive IFN-γ-secreting cells in vitreous and PBMCs	IFN-γ-ELISpot assay	Not detectable for UW-LNP-ABE8E

Legend: All specifications are relative to a sham vehicle control unless otherwise indicated.

We will deliver 200 µg (4 eyes) or 300 µg (4 eyes) of DS in a 100 µl injection volume[9–11,38]. Signs of retinal toxicity include the disruption of RPE, vascular occlusions, macular and retinal edema, crystalline deposition, and inflammation. Subtle changes in spectral domain optical coherence tomography (SD-OCT), fundus autofluorescence, or multifocal ERG before drug administration and a week after drug administration will assess clinical or subclinical toxicity. Both full-field and multifocal ERG will be performed before and 2-, 4-, and 8-weeks after subretinal delivery using standard ISCEV protocols. The immunogenicity of UW-LNP-ABE8E will also be assessed via blood analysis at different time points as well as tissue analysis at the termination of the

experiment as described in **Table 5**. This study will be used to inform the dose levels for subsequent GLP toxicity studies in NHP.

5.1.17. GLP Safety and Biodistribution of UW-LNP-ABE8E

Safety and biodistribution studies in rats and NHP will be conducted by a contracted CRO in compliance with FDA GLP using engineering-grade or GMP-grade UW-LNP-ABE8E. Specific details regarding these proposed, definitive GLP toxicity and biodistribution studies will be included for discussion in the pre-IND meeting.

5.2. Quality Background Information

5.2.1. Drug Product

UW-LNP-ABE8E is a Cas-based adenine base editor, ABE8E, paired with either a guide RNA targeting *KCNJ13* mutation W53X or guide RNA targeting *KCNJ13* mutation T153I, each of which causes LCA16. The DS is delivered to the RPE of LCA16 patients by a novel LNP delivery system via subretinal injection. UW-LNP-ABE8E is generated by admixing the RNA and LNP components (**Figure 17**) under shear while vortexing or using a fluidic mixer. The resulting solution is dialyzed, concentrated, and filtered prior to formulation, fill and finish **(Figure 18)**. We anticipate that the final DP will be formulated, filled and finished in a cryovial or ISO 2R glass vial, frozen and stored at -80° C. The details of the DP, the container closure and labeling will be included in the pre-IND package.

[redacted]

5.2.2. Dose Preparation

The drug product will be formulated in an injection-ready format. To administer UW-LNP-ABE8E, the DP vial will be thawed and warmed to room temperature by clinical site staff at the point-of-care just prior to patient injection.

5.2.3. Excipients and Ancillary Materials

As a novel lipid nanoparticle complex containing mRNA encoding an adenine base editor and guide RNA, UW-LNP-ABE8E has a manufacturing process involving several key components (**Table 6**). Excipients used to [redacted] which will be sourced from contract manufacturers and accompanied by Certificates of Analysis detailing sufficient quality for their use in the manufacture of UW-LNP-ABE8E. Certificates of Analysis will be documented and retained for any materials used for nonclinical studies that support IND submission. These lipid components will be tested and released for use in a GMP-compliant manufacturing facility. The manufacturing process for the [redacted] **Figure 19**)[39] will be transferred to a CDMO and characterized according to the description in Section 5.2.4.

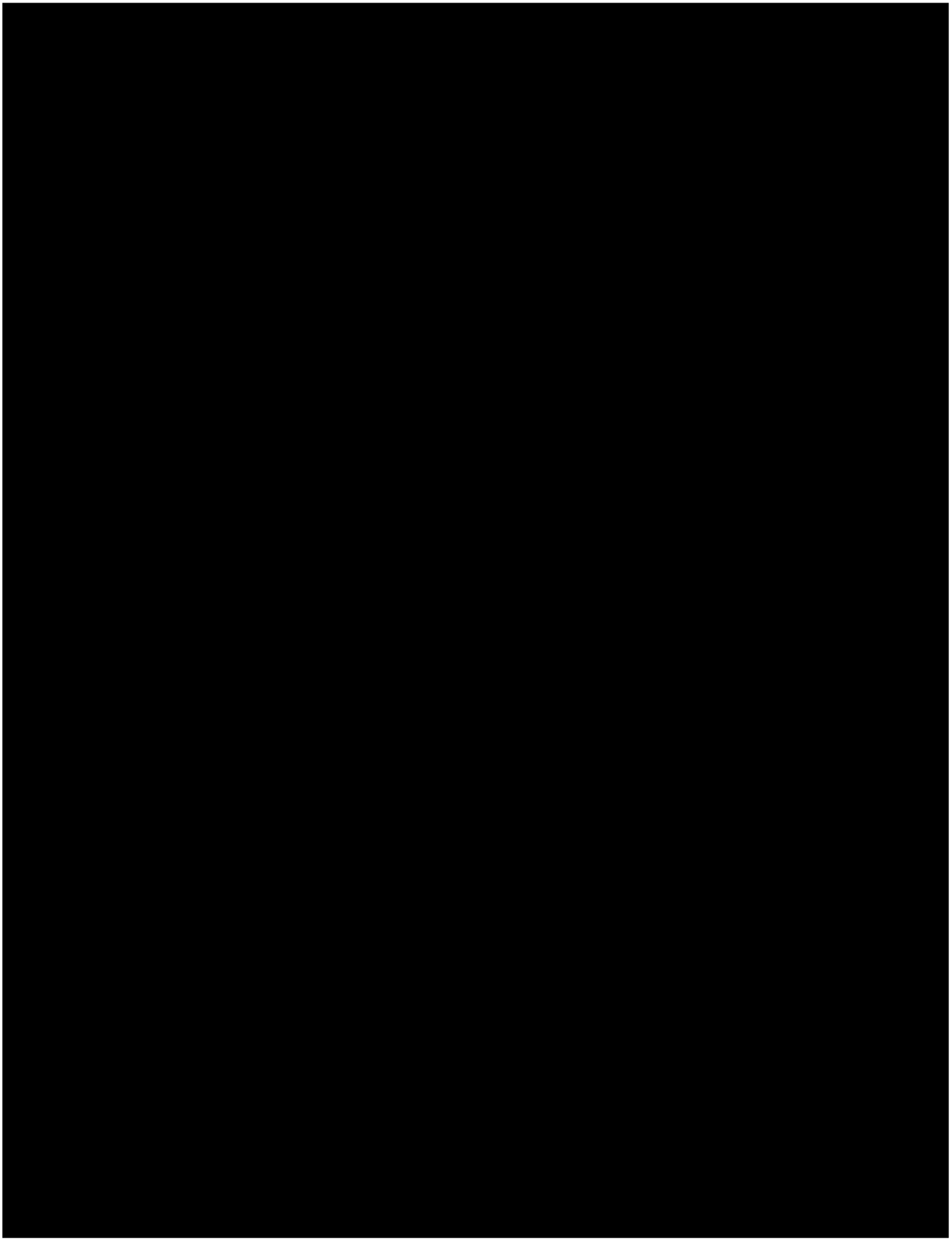

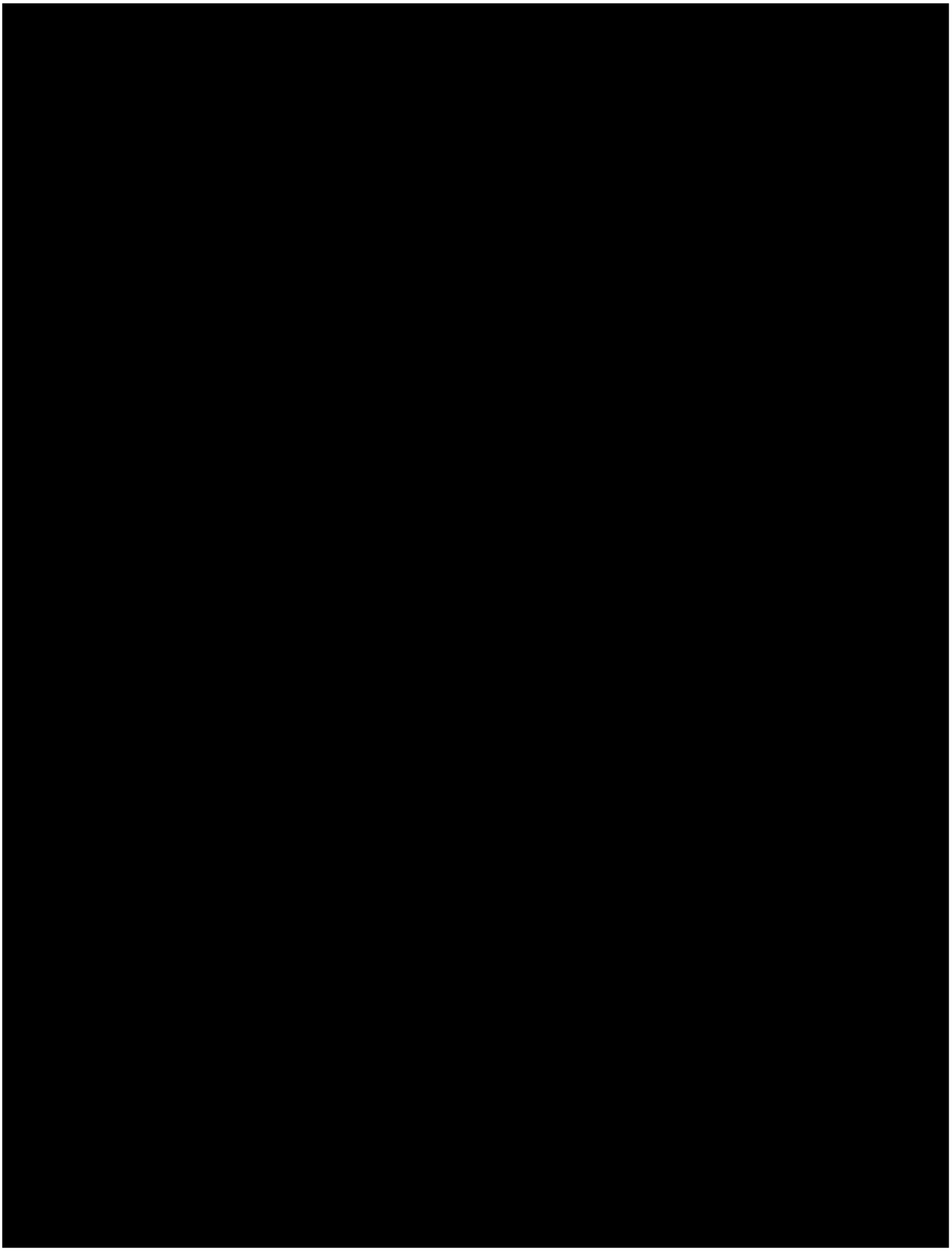

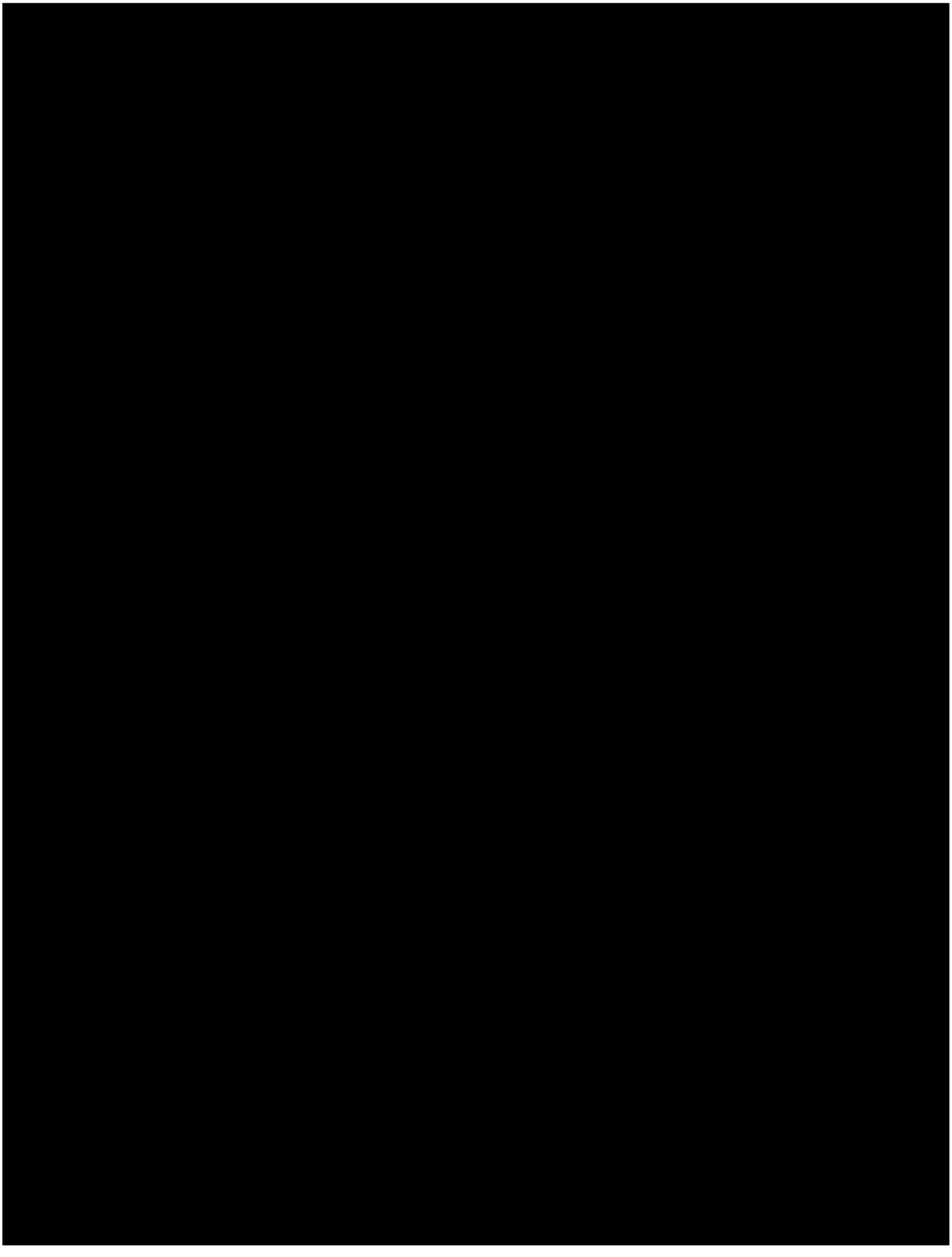

5.2.5. Drug Substance

5.2.5.1 Single-guide RNA (sgRNA)

5.2.5.1.1 sgRNA Manufacturer

The sgRNA will be generated by an industry-recognized vendor that the UW CRISPR Vision Program has identified. Contract negotiations are in process.

5.2.5.1.2 General Method of Preparation of sgRNA

The sgRNA will be prepared using solid phase, phosphoramidite-based oligonucleotide synthesis, either all-in-one inline synthesis or by enzymatic ligation of smaller fragments. Both approaches are consistent with the synthetic methods used for other FDA-approved oligonucleotide drugs.[52,53] We have entered into discussions with two industry-recognized vendors for sgRNA DS synthesis. Both vendors offer GMP-like IND Enabling Guides, produced in a controlled but non-classified facility, as well as fully compliant GMP facilities to enable rapid

transition to later stage clinical trials with simple technology transfer. One vendor uses inline synthesis to produce full-length sgRNA guides. They have a default product purity of 70% and use HPLC and mass spectrometry as part of quality control. Solid phase extraction, buffer exchange and residual solvents can influence the purity of the resulting sgRNA produced. With a qualified protocol they may be able to reach a 90-95% purity. Another vendor uses the ligation of smaller oligonucleotides to produce full-length sgRNA guides. The ligation method inherently selects for intact fragments and facilitates the HPLC-based purification of full-length guide, allowing them to reach 95-97% purity. After performing endotoxin and bioburden testing, sgRNAs, like other modified oligonucleotides, will be stored for up to 3 years lyophilized at -20 C.

5.2.5.2 Adenine Base Editor 8E mRNA (ABE8E mRNA)

5.2.5.2.1 ABE8E mRNA Manufacturer

The adenine base editor, ABE8E, will be generated by an industry-recognized vendor that the UW CRISPR Vision Program has identified. Contract negotiations are in process.

5.2.5.2.2 General Method of Preparation of ABE8E mRNA

We plan to use an industry-recognized vendor for the manufacture of ABE8E mRNA to help support drug product synthesis and delivery. A variety of assays will be used to support product identification, purity, characterization, impurity quantification, safety, and qualitative assessment, including USP osmolality, pH, gel and capillary electrophoresis, HPLC, and Sanger and long-read sequencing.

5.2.5.3 Drug Substance Release Testing

The phase-appropriate sgRNA and ABE8E will be generated by an industry-recognized vendor, with whom the UW CRISPR Vision Program will work closely to identify the necessary release tests required. The draft proposed release testing for the final DS is shown in **Table 11** and **Table 12** for the sgRNA and ABE8E mRNA, respectively. Samples for these tests will be taken from the batch of single-use vials after fill/finish. Based on batch size, vials for sterility will be taken from the start, middle and end of filling. If cryopreservation is deemed necessary at the end of fill/finish and is also considered to impact the results of a particular test, samples will be taken prior to cryopreservation and kept refrigerated until assayed.

Table 11 sgRNA Release Testing

Test	Method	Acceptance Criteria
Appearance	Visual	White to off-white solid and free from foreign matter
Identity	MS	Matches theoretical molecular weight within 0.05% error
Purity	Ion Exchange (IE)-HPLC	Purity ≥ 90%
Moisture Content	Karl Fischer USP <921> Ph. Eur. 2.5.32	NMT 10%
Sodium Content	ICP MS USP <233> Ph. Eur. 2.5.20	NMT 8%
Endotoxin	USP <85> Ph. Eur. 2.6.14 kinetic turbidimetric method	NMT 0.09 EU/mg
Microbial enumeration	USP <61> Ph. Eur. 2.6.12	NMT 100 cfu/g TAMC NMT 100 cfu/g TYMC

Legend: The proposed release testing will verify the identity and purity of the DS sgRNA prior to use. A series of assays will be conducted to examine key attributes of the DS, including visual appearance, molecular weight confirmation, purity, moisture and sodium content, endotoxin levels, and microbial enumeration. These assays will be conducted using samples taken from single-use vials after fill/finish, with sterility testing performed on vials collected at different stages of the filling process. If cryopreservation is required, additional samples will be taken before freezing to evaluate impacts on DS quality.

Table 12 ABE8E mRNA Characterization and Release Testing

Test	Method
Identification / PC / QA	Length/Purity/Integrity(smear analysis) - by fragment analyzer
Purity	mRNA Purity - by Ion Pair Reverse Phase HPLC Analysis
Impurity Quantification	Residual protein Routine - by NanoOrange
Impurity Quantification	Residual DNA by qPCR
QA	Residual dsRNA - by Dot Blot
Quantitative test of the active moiety	Concentration - by UV Spec (Absorbance at 260 nm)
PC	Poly A tail length - by LCMS
PC	Capping Assay - by LCMS
PC	Appearance - by USP <631>, USP <790>
PC	pH - by USP <791>
Safety (Microbial)	Endotoxin
Identification	Sanger sequencing
Safety (Microbial)	Bioburden
Identification / PC / QA	Enzymatic Digest - Base Composition LC/UV
Identification / PC / QA	Sequencing - Fingerprinting by LC/MS/MS
Identification / PC / QA	mRNA Identification - by RNA Agarose Gel
Identification	Protein Expression - by In vitro translation
Identification	RNase digestion
Identification	mRNA Identity - by RT-PCR
PC	Osmolality - by USP <785>
PC	Conductivity
QA	DNase & RNase Detection
Impurity Quantification	Residual NTP's
Quantitative tests for impurity content	Residual solvents
Safety (Microbial)	Sterility (late phase only)

Legend: Characterization and release testing are critical to ensure the identity, purity, and safety of the DS ABE8E mRNA. Analytical techniques will assess key attributes, including qualitative and quantitative evaluations of mRNA integrity, residual impurities, product characteristics, and microbial safety. PC: Product Characterization. QA: Qualitative Assessment

5.2.6. Drug Product Manufacturing Process

A high-level process flow diagram showing the current plan for manufacturing of UW-LNP-ABE8E DP is illustrated in **Figure 18**. UW-LNP-ABE8E will be manufactured from LNP components and the DS consisting of ABE8E mRNA and sgRNA.

5.2.7. Controlling Key UW-LNP-ABE8E Drug Product Attributes

The manufacturing process is designed with processes in place to maintain the safety, purity, identity, and potency of each UW-LNP-ABE8E product. The materials used will be phase-appropriate (**Table 6**) and facilities maintained at an appropriate cGMP level. The proposed DP release testing is shown in **Table 13**.

Table 13 UW-LNP-ABE8E Critical Quality Attributes and Release Assays

Attribute	Assay
Bioburden	Microbial enumeration
Appearance	Visual inspection

Identity	The chemical structure of LNP will be analyzed by FTIR
Payload Loading	RNA isolation and quantification
Strength	Weight of lyophilized or frozen product
pH	USP <791>
Particle Size	DLS
Zeta Potential	DLS
Purity Endotoxin	USP <771> - Limulus Amebocyte Lysate (LAL) kinetic turbidimetric assay
Osmolality	USP <785>
Sterility	USP <71>
Particulates	USP <788>
Potency	Reporter Cell Line Assay (Section 5.1.12)

Legend: The CQAs and corresponding assays for the UW-LNP-ABE8E formulation will ensure the safety, purity, identity, and potency of the DP. These assays will evaluate key attributes of UW-LNP-ABE8E, including bioburden, appearance, payload loading, particle size, and zeta potential, using methods including microbial enumeration, visual inspection, Fourier Transform Infrared Spectroscopy (FTIR), and Dynamic Light Scattering (DLS), respectively. Additional testing for endotoxins, osmolality, sterility, and particulates will ensure compliance with safety standards, and potency will be tested using a reporter cell line assay.

5.3. Preliminary Clinical Plan

The UW-LNP-ABE8E trial will be an open-label Phase 1/2 trial to demonstrate the safety and efficacy of subretinal injection of UW-LNP-ABE8E in LCA16 patients with W53X or T153I A-base mutations who are over 12 years-old and have viable RPE. A synopsis of the FIH clinical trial is provided in **Table 14**.

A single dose level (in a total dose volume of 300 µL, pending nonclinical safety data and DRF study) will first be tested in the worse eye of up to two (W53X) or four (T153I) patients, followed by injection in the contralateral eye approximately six weeks later. Injections in the first two patients for each mutation cohort will be staggered by six weeks. Before treatment of the contralateral eye, an assessment will be made as to whether pre-existing disease allows the contralateral eyes to be safely treated. The approximate 6-week interval for injection of the contralateral eye has been selected to allow for adequate safety monitoring following the first injection in the more severely affected eye and to allow for the possibility of successful treatment in the contralateral eye. It should be noted that for treatment to be successful, a patient must have sufficiently viable retinal cells, as per investigator assessment. Similarly, the LUXTURNA® package insert states that a patient must have viable retinal cells for treatment.

In all cases, subretinal bleb placement (up to three doses, totaling 300 µL) will be planned pre-operatively by the operating surgeon to provide the potential maximum benefit while minimizing the risk of adverse events. Efficacy endpoints will be measured via (1) performance in a multi-luminance mobility test (MLMT) course; (2) full-field stimulus testing (FST); (3) Best Corrected Visual Acuity (BCVA) testing as measured with the ETDRS (Early Treatment of Diabetic Retinopathy Study) chart; and (4) Full-field Electroretinography (ffERG) assessment using a standard International Society for Clinical Electrophysiology of Vision (ISCEV) protocol, as well as a c-wave assessment protocol. Exploratory endpoints may be added to help better understand the disease and its progression.

Given the extreme rarity of LCA16, with only 2-4 patients worldwide known to date with the two target mutations in *KCNJ13*, only a single dose level, which is projected to be a therapeutic dose of UW-LNP-ABE8E, in a single eye will be evaluated in the initial trial (**Table 14**). A traditional dose escalation program, in which one or more potentially non-therapeutic dose levels are tested, could preclude patients from subsequently receiving a demonstrated therapeutic dose in the same eye. In accordance with US draft FDA Guidance for Industry: Human Gene Therapy for Rare Diseases, the dose will be selected based on preclinical efficacy and nonclinical

toxicology data, to include the No Observed Adverse Effect Level (NOAEL) established during these preclinical toxicology studies. Following a suitable safety evaluation period, the contralateral eye of each patient may be treated.

All patients dosed with UW-LNP-ABE8E will be subsequently enrolled in a long-term follow-up study in compliance with US draft FDA Guidance for Industry: Long Term Follow-Up After Administration of Human Gene Therapy Products. The Sponsor plans to discuss the design of this trial with the Agency at the pre-IND meeting. Based on primary and secondary outcome measures, and the proposed monitoring plan.

Table 14 First-In-Human Clinical Trial Synopsis

Title	First-in-Human Base Editing for LCA16
Phase	Combined phase I/II
# of Trial Sites	One
# Subjects	Three
Patient Population	Leber Congenital Amaurosis 16 (LCA16), carrying a pathogenic W53X or T153I mutation, with clinical evidence of surviving RPE
Objectives	Therapeutic evaluation of UW-LNP-ABE8E
Investigational Product Dose	0.1 ml of UW-LNP-ABE8E by single subretinal injection
Control	Open label, single arm study
Population **Inclusion Criteria:** 1. Over the age of 12 and diagnosed with LCA16 containing a W53X or T153I mutation 2. Willing to provide informed consent and adhere to all study requirements 3. Clinical evidence of surviving RPE **Exclusion Criteria:** 1. Systemic disease 2. Previous medication 3. Prior eye surgeries/eye conditions 4. Other genetic diagnosis 5. Prior inclusion in any other investigational drug	
Criteria for Evaluation	**Primary Outcome Measures**: Increased light sensitivity by at least 0.1 log units by Multi-Luminance Mobility test. **Secondary Outcome Measures**: ERG showing rescue of both photopic and scotopic waveforms BCVA (± 5 letter change on the ETDRS chart) OCT demonstrating ellipsoid zone (EZ band-photoreceptor inner segment/outer segment junction)

6. LIST OF SPONSOR ATTENDEES

Attendee	Affiliation	Title
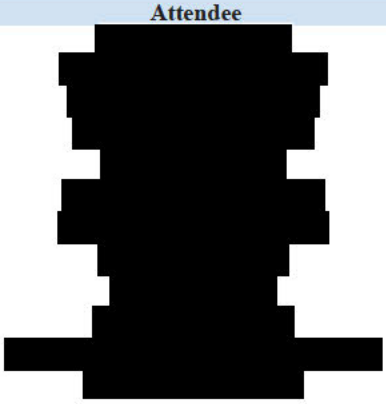	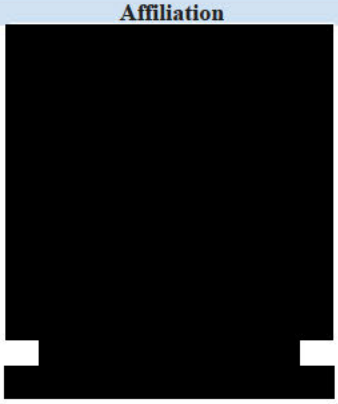	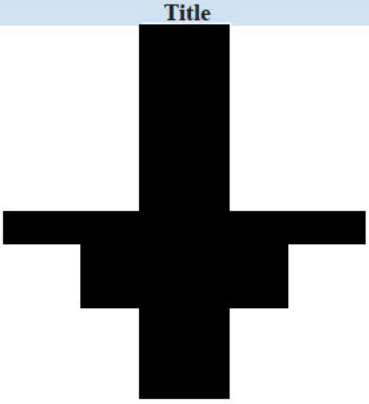

7. A LIST OF FDA STAFF ASKED TO PARTICIPATE IN THE REQUESTED MEETING

The participation of members of the Center for Biologics and Research Evaluation is requested.

8. SUGGESTED TELECONFERENCE DATE/TIMES

April 21-29 (any time, Monday, Tuesday, Thursday, Fridays preferred) or earlier

9. FORMAT OF THE MEETING

A teleconference is requested.

10. REFERENCES

1. Leber T. Ueber Retinitis pigmentosa und angeborene Amaurose. Arbeitsphysiologie. 1869 Dec 1;15(3):1–25.
2. Pattnaik BR, Shahi PK, Marino MJ, Liu X, York N, Brar S, Chiang J, Pillers DAM, Traboulsi EI. A Novel KCNJ13 Nonsense Mutation and Loss of Kir7.1 Channel Function Causes Leber Congenital Amaurosis (LCA16). Hum Mutat. 2015 Jul 1;36(7):720–727.
3. DiCarlo JE, Mahajan VB, Tsang SH. Gene therapy and genome surgery in the retina. J Clin Invest. 2018 Jun 1;128(6):2177–2188. PMCID: PMC5983345
4. Hwang GH, Park J, Lim K, Kim S, Yu J, Yu E, Kim ST, Eils R, Kim JS, Bae S. Web-based design and analysis tools for CRISPR base editing. BMC Bioinformatics. 2018;19(1):542. PMCID: PMC6307267
5. Siegner SM, Karasu ME, Schroder MS, Kontarakis Z, Corn JE. PnB Designer: a web application to design prime and base editor guide RNAs for animals and plants. BMC Bioinformatics. 2021;22(1):101. PMCID: PMC7923538
6. Shahi PK, Liu X, Aul B, Moyer A, Pattnaik A, Denton J, Pillers DAM, Pattnaik BR. Abnormal Electroretinogram after Kir7.1 Channel Suppression Suggests Role in Retinal Electrophysiology. Sci Rep. 2017 Sep 6;7(1):10651.
7. Shahi PK, Hermans D, Sinha D, Brar S, Moulton H, Stulo S, Borys KD, Capowski E, Pillers DM, Gamm DM, Pattnaik BR. Gene Augmentation and Readthrough Rescue Channelopathy in an iPSC-RPE Model of Congenital Blindness. Am J Hum Genet. 2019;104(2):310–318. PMCID: PMC6369573
8. Nork TM, Rasamison CM, Christian B, Murphy CJ. Emerging imaging technologies for assessing ocular toxicity in laboratory animals. In: Weir AB, Collins M, editors. Ocular Toxicity in Laboratory Animals: Molecular and Integrative Toxicology. New York: Springer; 2012.
9. Binley K, Widdowson PS, Kelleher M, de Belin J, Loader J, Ferrige G, Carlucci M, Esapa M, Chipchase D, Angell-Manning D, Ellis S, Mitrophanous K, Miskin J, Bantseev V, Nork TM, Miller P, Naylor S. Safety and biodistribution of an equine infectious anemia virus-based gene therapy, RetinoStat((R)), for age-related macular degeneration. Hum Gene Ther. 2012;23(9):980–991. PMID: 22716662
10. Ye GJ, Budzynski E, Sonnentag P, Nork TM, Miller PE, Sharma AK, Ver Hoeve JN, Smith LM, Arndt T, Calcedo R, Gaskin C, Robinson PM, Knop DR, Hauswirth WW, Chulay JD. Safety and Biodistribution Evaluation in Cynomolgus Macaques of rAAV2tYF-PR1.7-hCNGB3, a Recombinant AAV Vector for Treatment of Achromatopsia. Hum Gene Ther Clin Dev. 2016;27(1):37–48. PMCID: PMC4851175
11. Ye GJ, Budzynski E, Sonnentag P, Nork TM, Sheibani N, Gurel Z, Boye SL, Peterson JJ, Boye SE, Hauswirth WW, Chulay JD. Cone-Specific Promoters for Gene Therapy of Achromatopsia and Other Retinal Diseases. Hum Gene Ther. 2016 Jan;27(1):72–82. PMID: 26603570
12. Hernandez CC, Gimenez LE, Dahir NS, Peisley A, Cone RD. The unique structural characteristics of the Kir 7.1 inward

rectifier potassium channel: a novel player in energy homeostasis control. Am J Physiol Cell Physiol. American Physiological Society; 2023 Mar 1;324(3):C694–C706. PMCID: PMC10026989

13. Bok D. The retinal pigment epithelium: a versatile partner in vision. J Cell Sci Suppl. England; 1993;17:189–195. PMID: 8144697
14. Sparrow JR, Hicks D, Hamel CP. The retinal pigment epithelium in health and disease. Curr Mol Med. Netherlands; 2010 Dec;10(9):802–823. PMCID: PMC4120883
15. Strauss O. The retinal pigment epithelium in visual function. Physiol Rev. United States; 2005 Jul;85(3):845–881. PMID: 15987797
16. Beverley KM, Shahi PK, Kabra M, Zhao Q, Heyrman J, Steffen J, Pattnaik BR. Kir7.1 disease mutant T153I within the inner pore affects K^+ conduction. Am J Physiol Cell Physiol. American Physiological Society; 2022 Jul 1;323(1):C56–C68.
17. Richter MF, Zhao KT, Eton E, Lapinaite A, Newby GA, Thuronyi BW, Wilson C, Koblan LW, Zeng J, Bauer DE, Doudna JA, Liu DR. Phage-assisted evolution of an adenine base editor with improved Cas domain compatibility and activity. Nat Biotechnol. 2020 Jul;38(7):883–891. PMCID: PMC7357821
18. Davis JR, Wang X, Witte IP, Huang TP, Levy JM, Raguram A, Banskota S, Seidah NG, Musunuru K, Liu DR. Efficient in vivo base editing via single adeno-associated viruses with size-optimized genomes encoding compact adenine base editors. Nat Biomed Eng. Nature Publishing Group; 2022 Jul 28;1–12. PMID: 35902773
19. Matet A, Kostic C, Bemelmans AP, Moulin A, Rosolen SG, Martin S, Mavilio F, Amirjanians V, Stieger K, Lorenz B, Behar-Cohen F, Arsenijevic Y. Evaluation of tolerance to lentiviral LV-RPE65 gene therapy vector after subretinal delivery in non-human primates. Transl Res. Elsevier BV; 2017 Oct;188:40–57.e4.
20. Foldvari M, Chen DW, Nafissi N, Calderon D, Narsineni L, Rafiee A. Non-viral gene therapy: Gains and challenges of non-invasive administration methods. J Control Release. Elsevier BV; 2016 Oct;240:165–190.
21. Kaiser J. Gene therapy field hit by fresh safety concern. Science. American Association for the Advancement of Science (AAAS); 2018 Feb 9;359(6376):621–621.
22. Chancellor D, Barrett D, Nguyen-Jatkoe L, Millington S, Eckhardt F. The state of cell and gene therapy in 2023. Mol Ther. 2023 Dec 6;31(12):3376–3388. PMCID: PMC10727993
23. Park H, Park K, Shalaby WSW. Biodegradable Hydrogels for Drug Delivery. CRC Press; 2011.
24. National Academies of Sciences, Engineering, and Medicine, Health and Medicine Division, Board on Population Health and Public Health Practice, Committee on Community-Based Solutions to Promote Health Equity in the United States. Communities in Action: Pathways to Health Equity. National Academies Press; 2017.
25. Ramsay E, Lajunen T, Bhattacharya M, Reinisalo M, Rilla K, Kidron H, Terasaki T, Urtti A. Selective drug delivery to the retinal cells: Biological barriers and avenues. J Control Release. Elsevier BV; 2023 Sep 1;361:1–19. PMID: 37481214
26. Kabra M, Shahi PK, Wang Y, Sinha D, Spillane A, Newby GA, Saxena S, Tong Y, Chang Y, Abdeen AA, Edwards KL, Theisen CO, Liu DR, Gamm DM, Gong S, Saha K, Pattnaik BR. Nonviral base editing of KCNJ13 mutation preserves vision in a model of inherited retinal channelopathy. J Clin Invest [Internet]. American Society for Clinical Investigation; 2023 Oct 2;133(19). Available from: https://www.jci.org/articles/view/171356 PMCID: PMC10541187
27. Smith RS, Rudt LA. Ocular vascular and epithelial barriers to microperoxidase. Invest Ophthalmol. Invest Ophthalmol; 1975 Jul;14(7):556–560. PMID: 806549
28. Huang TP, Heins ZJ, Miller SM, Wong BG, Balivada PA, Wang T, Khalil AS, Liu DR. High-throughput continuous evolution of compact Cas9 variants targeting single-nucleotide-pyrimidine PAMs. Nat Biotechnol. Springer Science and Business Media LLC; 2023 Jan;41(1):96–107. PMCID: PMC9849140
29. Toms M, Dubis AM, Lim WS, Webster AR, Gorin MB, Moosajee M. Missense variants in the conserved transmembrane M2 protein domain of KCNJ13 associated with retinovascular changes in humans and zebrafish. Exp Eye Res. Elsevier BV; 2019 Dec;189(107852):107852. PMCID: PMC6899441
30. Levy D, Zayat M. The Sol-Gel Handbook: Synthesis, Characterization, and Applications. John Wiley & Sons; 2015.
31. Wang Y, Shahi PK, Wang X, Xie R, Zhao Y, Wu M, Roge S, Pattnaik BR, Gong S. In vivo targeted delivery of nucleic acids and CRISPR genome editors enabled by GSH-responsive silica nanoparticles. J Control Release. 2021 Aug 10;336:296–309. PMCID: PMC8383466
32. [cited 2025 Feb 12]. Available from: https://www.fda.gov/media/156894/download

33. 007914 - Ai14 , Ai14D or Ai14(RCL-tdT)-D Strain Details [Internet]. [cited 2025 Feb 12]. Available from: https://www.jax.org/strain/007914
34. Yin W, Kim HT, Wang S, Gunawan F, Wang L, Kishimoto K, Zhong H, Roman D, Preussner J, Guenther S, Graef V, Buettner C, Grohmann B, Looso M, Morimoto M, Mardon G, Offermanns S, Stainier DYR. The potassium channel KCNJ13 is essential for smooth muscle cytoskeletal organization during mouse tracheal tubulogenesis. Nat Commun. Nat Commun; 2018 Jul 19;9(1):2815. PMCID: PMC6052067
35. Katti A, Foronda M, Zimmerman J, Diaz B, Zafra MP, Goswami S, Dow LE. GO: a functional reporter system to identify and enrich base editing activity. Nucleic Acids Res. Oxford University Press (OUP); 2020 Apr 6;48(6):2841–2852. PMCID: PMC7102966
36. St Martin A, Salamango D, Serebrenik A, Shaban N, Brown WL, Donati F, Munagala U, Conticello SG, Harris RS. A fluorescent reporter for quantification and enrichment of DNA editing by APOBEC-Cas9 or cleavage by Cas9 in living cells. Nucleic Acids Res. Oxford Academic; 2018 Aug 21;46(14):e84. PMCID: PMC6101615
37. Bantseev V, Miller PE, Nork TM, Rasmussen CA, McKenzie A, Christian BJ, Booler H, Thackaberry EA. Determination of a No Observable Effect Level for Endotoxin Following a Single Intravitreal Administration to Cynomolgus Monkeys. J Ocul Pharmacol Ther. 2019;35(4):245–253. PMCID: PMC7141559
38. Nork TM, Murphy CJ, Kim CB, Ver Hoeve JN, Rasmussen CA, Miller PE, Wabers HD, Neider MW, Dubielzig RR, McCulloh RJ, Christian BJ. Functional and anatomic consequences of subretinal dosing in the cynomolgus macaque. Arch Ophthalmol. 2012;130(1):65–75. PMCID: PMC3254795
39. Zhu M, Wang X, Xie R, Wang Y, Xu X, Burger J, Gong S. Guanidinium-rich lipopeptide-based nanoparticle enables efficient gene editing in skeletal muscles. ACS Appl Mater Interfaces. American Chemical Society (ACS); 2023 Mar 1;15(8):10464–10476. PMID: 36800641
40. Fitch CA, Platzer G, Okon M, Garcia-Moreno BE, McIntosh LP. Arginine: Its pKa value revisited. Protein Sci. Wiley; 2015 May;24(5):752–761. PMCID: PMC4420524
41. Wexselblatt E, Esko JD, Tor Y. On guanidinium and cellular uptake. J Org Chem. American Chemical Society (ACS); 2014 Aug 1;79(15):6766–6774. PMCID: PMC4120969
42. Heyda J, Okur HI, Hladílková J, Rembert KB, Hunn W, Yang T, Dzubiella J, Jungwirth P, Cremer PS. Guanidinium can both Cause and Prevent the Hydrophobic Collapse of Biomacromolecules. J Am Chem Soc. 2017 Jan 18;139(2):863–870. PMCID: PMC5499822
43. Pantos A, Tsogas I, Paleos CM. Guanidinium group: a versatile moiety inducing transport and multicompartmentalization in complementary membranes. Biochim Biophys Acta. Elsevier BV; 2008 Apr;1778(4):811–823. PMID: 18178146
44. Rothbard JB, Jessop TC, Lewis RS, Murray BA, Wender PA. Role of membrane potential and hydrogen bonding in the mechanism of translocation of guanidinium-rich peptides into cells. J Am Chem Soc. American Chemical Society (ACS); 2004 Aug 11;126(31):9506–9507. PMID: 15291531
45. Rothbard JB, Jessop TC, Wender PA. Adaptive translocation: the role of hydrogen bonding and membrane potential in the uptake of guanidinium-rich transporters into cells. Adv Drug Deliv Rev. Elsevier BV; 2005 Feb 28;57(4):495–504. PMID: 15722160
46. A Boronic Acid−Rich Dendrimer with Robust and Unprecedented Efficiency for Cytosolic Protein Delivery and CRISPR.
47. Barrios A, Estrada M, Moon JH. Carbamoylated guanidine-containing polymers for non-covalent functional protein delivery in serum-containing media. Angew Chem Weinheim Bergstr Ger [Internet]. Wiley; 2022 Mar 14;134(12). Available from: http://dx.doi.org/10.1002/ange.202116722
48. Chang H, Lv J, Gao X, Wang X, Wang H, Chen H, He X, Li L, Cheng Y. Rational design of a polymer with robust efficacy for intracellular protein and peptide delivery. Nano Lett. American Chemical Society (ACS); 2017 Mar 8;17(3):1678–1684.
49. Guo S, Huang Q, Wei J, Wang S, Wang Y, Wang L, Wang R. Efficient intracellular delivery of native proteins facilitated by preorganized guanidiniums on pillar[5]arene skeleton. Nano Today. Elsevier BV; 2022 Apr;43(101396):101396.
50. Helical Polypeptides Bearing HydrophobicAmino Acid Pendants for Efficient Gene Delivery.
51. Agmatine-Grafted Bioreducible Poly (l-Lysine) for GeneDelivery with Low Cytotoxicity and High Efficiency.
52. Egli M, Manoharan M. Chemistry, structure and function of approved oligonucleotide therapeutics. Nucleic Acids Res. 2023 Apr 11;51(6):2529–2573. PMCID: PMC10085713

53. Obexer R, Nassir M, Moody ER, Baran PS, Lovelock SL. Modern approaches to therapeutic oligonucleotide manufacturing. Science. 2024 Apr 12;384(6692):eadl4015. PMID: 38603508